

**EVALUATION OF RESERVOIR PROPERTIES AND
SUBSURFACE STRUCTURAL INTERPRETATION OF
MIANO FIELD, CENTRAL INDUS BASIN PAKISTAN**



By

**Adnan Ahmad
Kaleem Tahir Choudhry**

**Department of Earth and Environmental Sciences
Bahria University, Islamabad**

2023

**EVALUATION OF RESERVOIR PROPERTIES AND
SUBSURFACE STRUCTURAL INTERPRETATION OF
MIANO FIELD, CENTRAL INDUS BASIN PAKISTAN**



A thesis submitted to Bahria University, Islamabad in partial fulfillment
of the requirement for the degree of B.S in Geophysics.

By

**Adnan Ahmad
Kaleem Tahir Choudhry**

**Department of Earth and Environmental Sciences
Bahria University, Islamabad**



2023

Bahria University
Department of Earth & Environmental Sciences
Islamabad Campus, Islamabad

Dated: 13/02/2023

Certificate

This thesis is submitted by **Mr. Adnan Ahmad** and **Mr. Kaleem Tahir Chaudhry** is accepted in the present form by Department of Earth & Environmental Sciences, Bahria University, Islamabad as the partial fulfillment of the requirement for the degree of **Bachelor of Sciences in Geophysics**, 4 years program (Session 2018– 2022).

Committee Members	Name	Signature
Supervisor	Mr. M. Raiees Amjad	
Internal Examiner	Dr. Muhsan Ehsan	
External Examiner	Mr. Muyassar Hussain	
Head of Department (E&ES)	Dr. Said Akbar Khan	

ABSTRACT

The current study's goal is to use seismic and well data to better understand the underlying geology and hydrocarbon potential of the Miano region. On eight seismic lines, subsurface structural interpretation has been carried out. Well-to-seismic tie distinguished three distinct horizons, namely Habib Rahi (Eocene), Upper Goru Formation (Cretaceous), and Lower Goru Formation (Cretaceous). Normal faults are interpreted which are forming horst and graben structures as a result of extensional tectonic settings. Petrophysical study was carried out on the well logs of Miano-02. Based on wireline log data, one hydrocarbon bearing zones was found in the Lower Goru Formation. Various Petrophysical parameters, such as we examine reservoir parameters, the amount of shale, average and effective porosities, and hydrocarbon saturation were computed. The thickness of hydrocarbon bearing zones is 3m (Miano-02) with calculated shale volumes of 7.483% The effective porosities and hydrocarbon saturation of the corresponding zones are determined to be 10.556% (Miano-02), and 37.073%. Lastly, pore pressure prediction within the Lower Goru Formation has been carried out using the Eaton's method to identify the abnormal pressure intervals. The evaluation of the pore pressure shows that there is overpressure in the top part (2226-3000m) of the Lower Goru Formation, which may make drilling difficult. The lowest half of the formation, on the other hand, possesses drillable pressure conditions.

ACKNOWLEDGEMENTS

We would like to express our heartfelt gratitude to Mr. Muhammad Raiees Amjad, Assistant Professor, Department of Earth & Environmental Sciences, Bahria University Islamabad, for his immense support and guidance that we needed to carry out this important task. We are very grateful for his caring assistance and critique during the whole research.

We would also like to deliver our appreciation to Head of Department, Earth and Environmental Sciences, for providing us the Geophysical Software lab facility to perform our research work. A special thanks to all the teachers for their constant support throughout the degree. We are fortunate to have our parents by our sides, who have always provided financial and moral support as well as assisted us in finishing this assignment and our degree programed.

Our thanks also go to DGPC and LMKR for providing us with pubic domain data for the research. We would also like to thank LMK Resources of Pakistan for providing the GVERSE software to Bahria University under their University Grant program to complete this research work.

TABLE OF CONTENTS

ABSTRACT	i
ACKNOWLEDGEMENTS	ii
TABLE OF CONTENTS	iii
FIGURES	vi
TABLES	7

CHAPTER 1

INTRODUCTION

1.1	Study location	8
1.2	Accessibility and Terrain	9
1.3	Climate	9
1.4	Objectives.....	9
1.5	Miano Field Exploration History	9
1.5.1	Literature Review	10
1.6	Available Data	10
1.7	Methodology	11

CHAPTER 2

THE GEOGRAPHY OF THE AREA

2.1	Pakistan's Sedimentary Basin.....	13
2.2	Central Indus Basin	13
2.2.1	Punjab Platform	14
2.2.2	Sulaiman Depression.....	14
2.2.3	Sulaiman Fold Belt	14
2.3	Petroleum System, Tectonics and Stratigraphy	15
2.3.1	The Region's Tectonic	15
2.3.2	Regions Structural Setting	17
2.3.3	Stratigraphy of the Central Indus Basin	17
2.3.3.1	Sembar Formation	19
2.3.3.2	Goru Formation	19
2.3.3.3	Parh Formation	20
2.3.3.4	Pab Sandstone	20
2.3.3.5	Kirthar Formation:.....	20
2.3.3.6	Drazinda Member:.....	20
2.3.3.7	Pirkoh Member:	21

2.3.3.8	Sirki Member:	21
2.3.3.9	Habib Rahi Member:	21
2.3.3.10	Ghazij Member:	21
2.3.3.11	Sui Main Limestone:	21
2.3.3.12	Ranikot Formation:.....	21
2.4	Petroleum System	22
2.4.1	Source Rocks	22
2.4.2	Reservoir Rocks.....	22
2.4.3	Seal Rocks.....	23
2.4.4	Traps.....	23

CHAPTER 3

SEISMIC DATA INTERPRETATION

3.1	Introduction.....	25
3.2	Seismic Data	25
3.3	Base Map.....	26
3.4	Time Depth Chart	27
3.5	Picking of Horizon.....	28
3.6	Fault Picking and Correlation	29
3.7	Interpretation of Seismic Lines	29
3.7.1	Interpretation of P2092-113.....	29
3.7.2	Interpretation of P2092-111.....	29
3.7.3	Interpretation of P2092-115.....	31
3.7.4	Interpretation of P2092-117.....	31
3.7.5	Interpretation of P2092-119.....	32
3.7.6	Interpretation of P2092-121.....	32
3.7.7	Interpretation of P2092-114.....	34
3.7.8	Interpretation of P2092-116.....	34
3.8	Mapping	34
3.8.1	Time Contour Maps.....	35
3.8.1.1	The Lower Goru Formation	35
3.8.1.2	The Upper Goru Formation.....	36
3.8.1.3	Habib Rahi Time Contour.....	37
3.8.2	Depth Contour Maps	39
3.8.2.1	Depth variation map of lower Goru:	39
3.8.2.2	Depth variation map of Upper Goru.....	40

3.8.2.3	Habib Rahi Depth Contour:	41
---------	---------------------------------	----

CHAPTER 4

PETROPHYSICAL ANALYSIS

4.1	Petrophysics	43
4.2	Wireline Log Interpretation Workflow	43
4.2.1	Volume of Shale (Vsh).....	44
4.3	Porosity.....	45
4.3.1	Density Porosity.....	45
4.3.2	Sonic Porosity	45
4.3.3	Average Porosity	46
4.3.4	Effective Porosity	46
4.4	Saturation of Water and Hydrocarbons.....	47
4.5	Pore Pressure Prediction	47
4.6	Basic Petrophysical analysis of Miano-02 well.....	49
4.6.1	Uninterpreted log curves	49
4.6.2	Petrophysical Results	52
4.11	Pore Pressure Prediction	53
4.7	Summation Table.....	55
CONCLUSIONS		57
REFERENCES		58

FIGURES

Figure 1.1. Describing the geographical position of the region.	8
Figure 1.2. Flowchart of methodologies adopted to evaluate the study area	11
Figure 2.1. Generalized regional tectonic map with location of major oil and gas fields in the study area.	15
Figure 2.2. Generalized tectonic map of the study area and adjoining regions in the Central Indus Basin. Study area is located on PanoAqil Graben in between Mari-Kandhkot Horst and Jacoababad-Kirthar Horst.	16
Figure 2.3. Generalized stratigraphy of Central Indus Basin	18
Figure 2.4. Study Area stratigraphy.	24
Figure 3.1. Seismic Interpretation Workflow adopted for the study.	26
Figure 3.2. Base Map of Miano area showing location of seismic lines and Miano-02 well.	27
Figure 3.3. Horizon picking based on the time depth chart of the Miano area.	28
Figure 3.4. Interpreted seismic section of line P2092-113.	30
Figure 3.5. Interpreted seismic section of line P2092-111	30
Figure 3.6. Interpreted seismic section of line P2092-115.	31
Figure 3.7. Interpreted seismic section of line P 2092-117	32
Figure 3.9. Interpreted seismic section of line P2092-121.	33
Figure 3.10. Interpreted seismic section of line P2092-114.	34
Figure 3.11. Interpreted seismic section of line P2092-116.	35
Figure 3.12. Time Contour Map of Lower Goru Formation in Miano field.	36
Figure 3.13 Time Contour Map of Upper Goru Formation in Miano field.	37
Figure 3.14. Time Contour Map of Habib Rahi Formation in Miano field.	38
Figure 3.15. Depth Contour Map of Lower Goru Formation in Miano field.	40
Figure 3.16. Depth Contour Map of Upper Goru Formation in Miano field.	41
Figure 3.17. Depth Contour Map of Habib Rahi Formation in Miano field.	42
Figure 4.1. Petrophysical Analysis Workflow adopted for the study.	44
Figure 4.2. Uninterpreted raw log curves of Miano-02 well.	51
Figure 4.3. Petrophysical Interpretation of Lower Goru Formation showing the zone of interest.	53
Figure 4.4. Estimation of pore pressures conditions in the Lower Goru Formation.	55

TABLES

Table 1.1. Data used for seismic and petrophysical analysis	11
Table 3.1. Time Depth chart prepared from the velocity window given at the seismic line.	28
Table 4.1. Summation table of Petrophysical Results of Miano-02 well.	56
Table 4.2. Summation table of Pore pressure prediction Results of Miano-02 well.	56

CHAPTER 1

INTRODUCTION

1.1 Study location

Miano is a gas field situated in the Central Indus Basin, which was discovered in 1993 and is known as Pakistan's first large stratigraphic trap. Covering an area of 814.02 km², it is located in the Thar desert, and is part of Block 20 in the northern half of the Lower Indus Basin. This block extends from the southern boundary of the Central Indus Basin towards the north and is situated south of Mari and north of the Kadanwari gas field. The Miano-02 well is the focus of the investigation and is situated between the Khairpur Jacobabad High and Kandkot High on the Panno Aqil Graben. The study area for the Miano-02 well is limited to 27° 24' 42.4" N latitude and 69° 19' 15.82" E longitude, and is dominated by the Cretaceous Extensional Fault, which trends NNW to SSE and is found in the Middle Indus Basin.

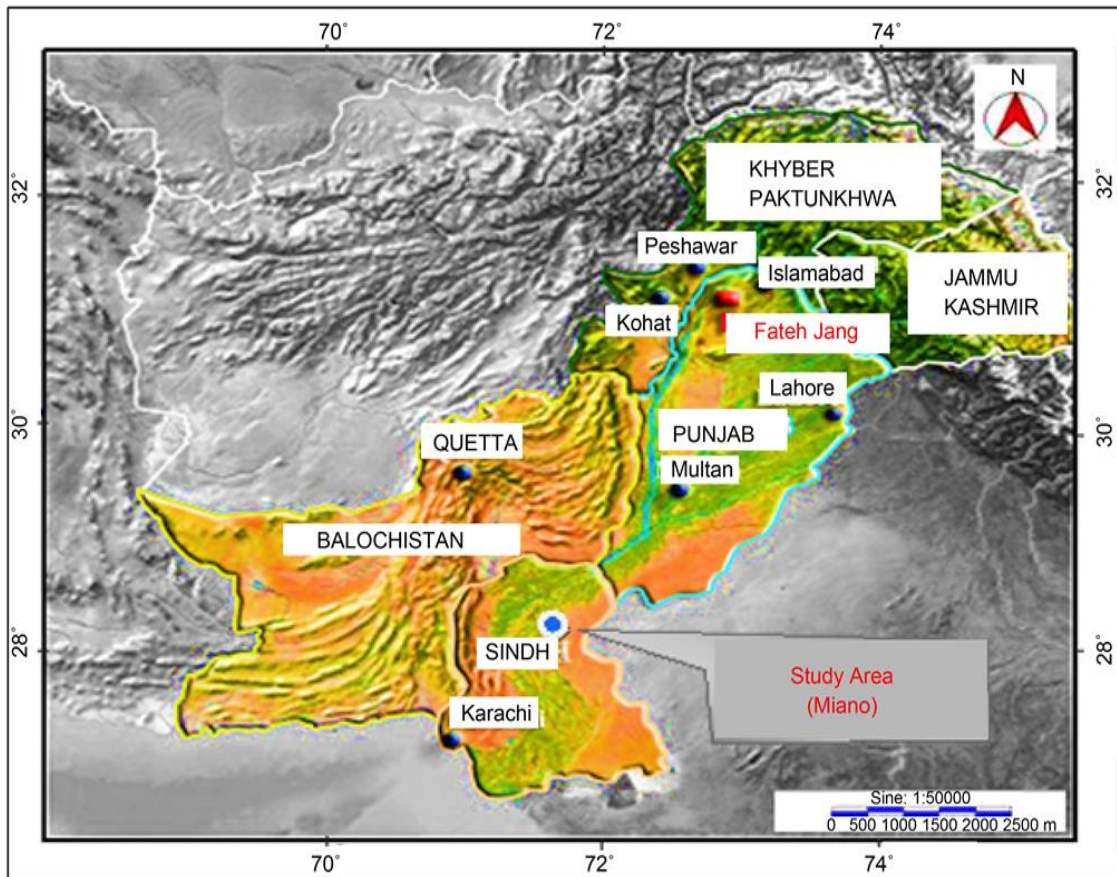


Figure 1.1. Describing the geographical position of the region (Naqi and Siddiqui, 2006).

The Maino-02 well was drilled with the primary aim of targeting the Lower Goru Formation A-Sands, which are from the Lower Cretaceous period. The well also had a secondary target, which was the Lower Goru Formation B-Sands from the same geological age. The total depth of the well was 3548.4m, and although the primary target did not yield any gas, gas was discovered in the secondary target.

1.2 Accessibility and Terrain

Miano is located in the district Sukkur, which is primarily covered with lush flora. The region is accessible by many routes that link to the district of Sukkur and eventually go to the Miano field area.

1.3 Climate

The Miano experiences a moderately tempered climate that is influenced by a consistent sea breeze that blows for eight months, from March to October. This sea breeze helps to moderate the typically hot temperatures, keeping them relatively cooler.

1.4 Objectives

The primary goal of the research is to assess the hydrocarbon potential of the region in the Central Indus Basin and delineate prospects using seismic and petrophysical techniques. This is accomplished by structurally interpreting accessible seismic lines. The essential portion of the aims was expressed in this structural research, which reflected a concept about the ideal places of hydrocarbon formation. Our dissertation's primary goals are as follows:

- (1) To comprehend the subsurface structure through the use of seismic and well data.
- (2) Locating hydrocarbon prospect regions at the reservoir level.
- (3) The seismic data from the region was studied to gain an understanding of the geological and tectonic history of the area.

1.5 Miano Field Exploration History

Sindh province is home to the Miano field. OMV, OGDCL, ENI, and others. PPL are the operator in Miano, with 17.68%, 52%, 15.16%, and 15% working interests, respectively. Miano was OMV Pakistan's first big breakthrough in 1993, followed by the Sawan Gas Field in District Khairpur in 1998.

OMV started drilling in 1993. The business has drilled 20 wells, nine of which have yielded gas finds. Miano raw gas is processed in the Kadanwari gas processing facility, which has been renovated in compliance with the joint use agreement agreed by the Miano and Kadanwari joint venture and the government. At the moment, the Kadanwari facility processes an average of 185MMsefd of Miano sales gas & Kadanwari, with an average gas sale from Miano field of 88MMsefd gas and 51 barrels' condensate. Total recoverable reserves comprise 492 Bef gas and 0.325 MM bbl. NGL. Pakistan Petroleum Limited.

1.5.1 Literature Review

Over the years, significant information on the regional and petroleum geology of the Middle Indus basin has been published in the Annual Technical Conferences hosted under the PAPG and SPE platforms. Peter (1997) published the first information on the Miano region, which explained the petroleum geology. The concept of stratigraphy and its relationship to hydrocarbon trapping has been explored in various studies.

One such study by Nadeem et al. (2004) outlines the criteria for comprehending sequence stratigraphy in the Sembar and Goru formations of the Middle Indus Basin. Additionally, Ibrahim (2007) and Afzal et al. (2009) have published research on the seismic inversion and sequence stratigraphy of the Goru "C" sand in the Sawan region, which provides valuable insights on this topic. These publications are thought-provoking and contribute to a better understanding of the relationship between stratigraphy and hydrocarbon trapping.

1.6 Available Data

The goal of this study is to understand the various stages involved in interpreting seismic reflection data in order to establish a correlation between the results derived from the seismic data and well logs such as the Sonic log, Resistivity log, Caliper log, Gamma ray log, Neutron log, and Density log.

Table 1.1. Data used for seismic and petrophysical analysis

Seismic data	Well data Miano 2
P2092-111	GR
P2092-113	SGR
P2092-115	SP
P2092-117	Neutron,
P2092-119	Density
P2092-121	Sonic
	Resistivity, Bit Size and Caliper.

In order to create a structural model of the research area, the HOD of Earth and Environmental Sciences at Bahria University Islamabad requested seismic reflection data and well log data (as shown in Table 1.1) from five seismic sections from the Directorate General of Petroleum Concessions, Government of Pakistan (DGPC) for the purpose of this study.

1.7 Methodology

The techniques used to achieve the study objectives are depicted.

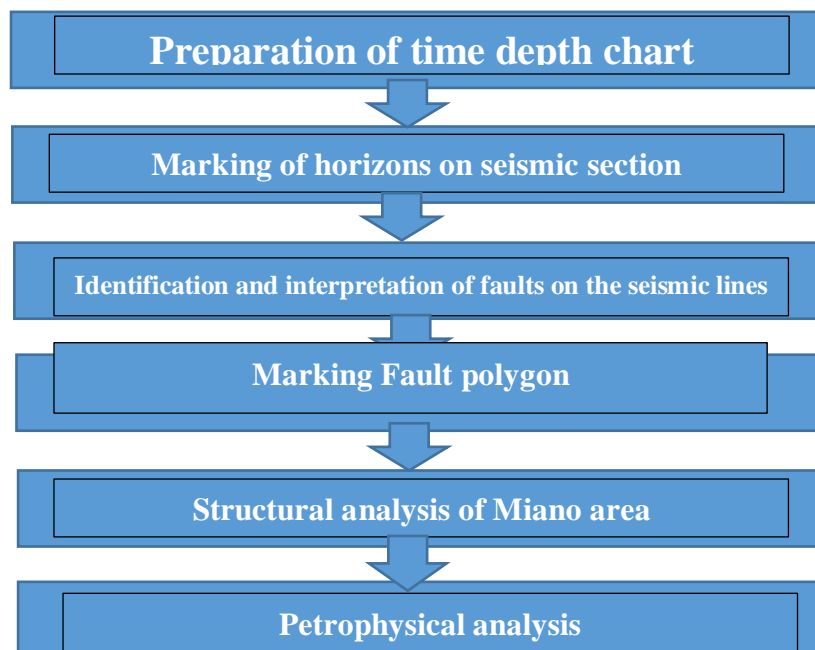


Figure 1.2. Flowchart of methodologies adopted to evaluate the study area

From the data provided by DGPC, first step was to create the Depth Chart from the time data to get the estimated depth of the horizons. Fault marking is the step that should be performed on the seismic data so that displacement / breakage can be observed while marking the horizons. By the comparison from different well data (Miano - 05 and Miano - 07) we can get the estimated time of our targeted horizons. Once the horizons are marked on the seismic lines, next step is to trace the faults along all the seismic lines i.e. the marking of fault polygon of our base map. As to find out the structural trend of the area and tectonic regime of the area Structural analysis is being done. After the seismic interpretation last step was to perform petrophysical analysis in which volume of shale, resistivity and pore pressure was carried out which is the main objective of thesis.

CHAPTER 2

THE GEOGRAPHY OF THE AREA

2.1 Pakistan's Sedimentary Basin

The geological history of Pakistan has resulted in the formation of two main sedimentary basins: the Indus Basin and the Baluchistan Basin, which were formed over different geological periods. The Pishin Basin, also known as the Kakar-Khorasan Basin, is a smaller basin that was recently discovered and is considered a middle basin. It formed due to the interaction between the Indian and Eurasian plates and was identified as the Median basin in a study conducted by Kadri in 1995. (Kadri, 1995)

The Indus basin has been subdivided into three sections:

- (i) Upper Indus Basin
- (ii) The Central Indus Basin
- (iii) Southern Indus Basin

2.2 Central Indus Basin

The Central Indus Basin is located in a complex tectonic setting that has been shaped by the collision of the Indian and Eurasian plates. The Indian plate is moving northwards and is currently colliding with the Eurasian plate along the Himalayan mountain range. The collision between these two plates has resulted in the uplift of the Himalayas and the formation of several other mountain ranges and plateaus in the region. The Central Indus Basin is located to the west of the Himalayas and is bordered by several mountain ranges, including the Hindu Kush to the northwest, the Karakoram to the northeast, and the Sulaiman Range to the southwest. The region is also affected by a number of active faults, including the Chaman Fault to the west and the Main Boundary Thrust to the east. These faults are responsible for the seismic activity in the region and have caused several earthquakes in the past, including the devastating earthquake that struck the city of Kashmir in 2005. The tectonic setting of the Central Indus Basin has also resulted in the formation of several oil and gas fields in the region, which are important sources of energy for Pakistan.

- (i) Punjab Platform
- (ii) Sulaiman Depression
- (iii) Sulaiman Fold belt

2.2.1 Punjab Platform

The broad monocline in the eastern part of the Central Indus Basin gradually slopes down into the Sulaiman Depression and lacks any visible surface outcrops of sedimentary rocks.. The Punjab Platform, situated at a greater distance from the collision zone, has undergone the least tectonic impact. Numerous wells have been drilled on this platform, aiding in the construction of a stratigraphic sequence that reveals some of Pakistan's most noteworthy stratigraphic pinch outs, according to Kadri (1995).

2.2.2 Sulaiman Depression

The Sulaiman Depression is a geological feature located in Pakistan that marks the eastern limit of the Balochistan Basin and the western limit of the Indus Basin. A major structural trough that runs in a north-south direction is present in the region, with the Sulaiman Range on the western side and the Kirthar Range on the eastern side acting as boundaries. The depression contains thick sedimentary deposits of Paleozoic, Mesozoic and Cenozoic age, and is an important hydrocarbon-producing region in Pakistan.

2.2.3 Sulaiman Fold Belt

The Sulaiman Fold Belt is a significant geological structure in the area, containing numerous anticlines spread across its expanse. (Kadri, 1995). Within the Kirthar and Sulaiman belts, there are a few large anticlines, mostly on the eastern side. Are unmistakably detachments. The Sulaiman Fold Belt is a geological feature located in Pakistan that extends from the Kohat Plateau in the north to the Arabian Sea in the south, covering an area of approximately 800 km in length and 200 km in width. It is a complex fold and thrust belt that was formed during the collision of the Indian and Eurasian tectonic plates in the Eocene-Oligocene period, approximately 35 to 55 million years ago. The Sulaiman Fold Belt consists of a series of parallel ridges and valleys that trend in a northwest-southeast direction, and is characterized by a thick sequence of sedimentary rocks, including sandstones, shales, limestones, and conglomerates. It is an important hydrocarbon-producing region in Pakistan, with significant reserves of natural gas and oil.

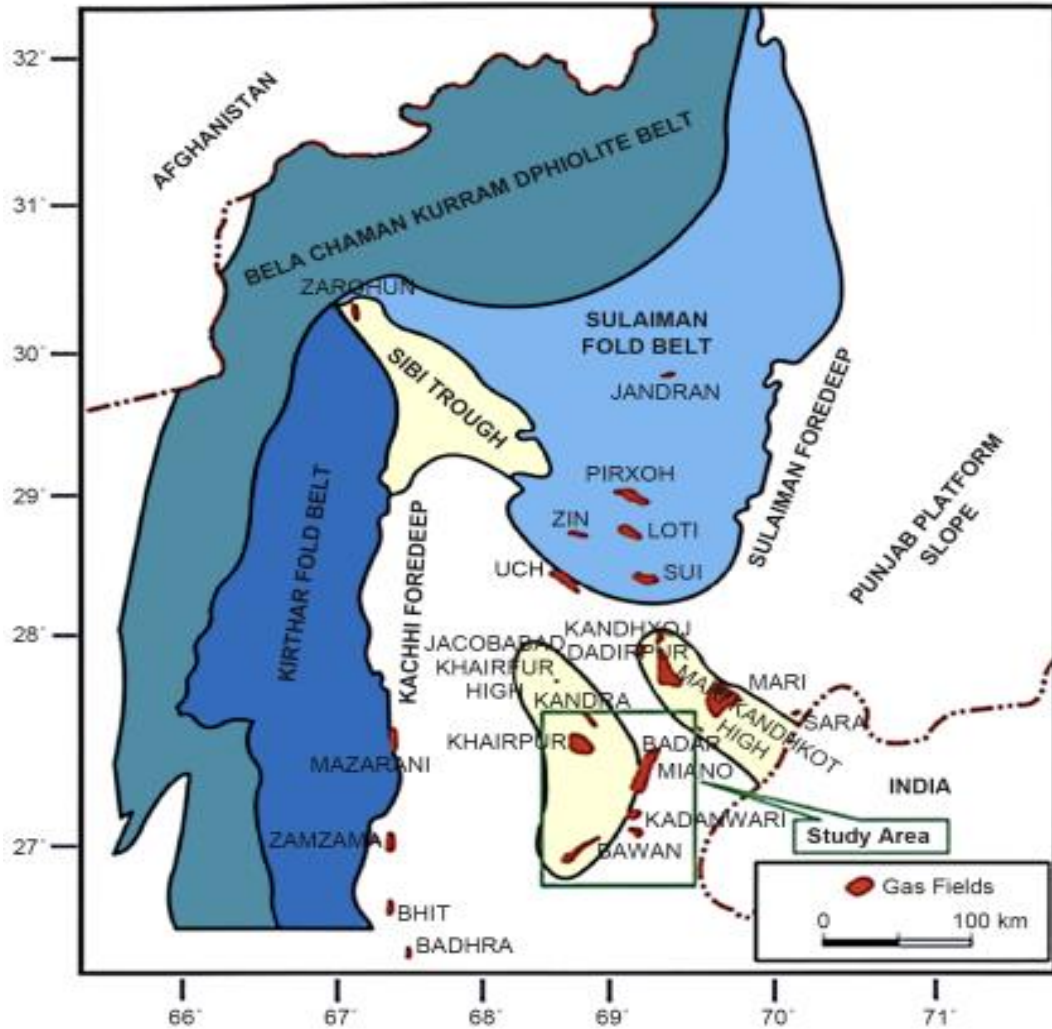


Figure 2.1. Generalized regional tectonic map with location of major oil and gas fields in the study area (modified after Ahmed et al., 2013)

2.3 Petroleum System, Tectonics and Stratigraphy

2.3.1 The Region's Tectonic

Miano block-20 is a low-lying region surrounded by two NW-SE running normal faults. Panno Aqil Graben is located between Kandkot Mari and Jacobabad-Kirthar Horsts. These horsts and graben formations are curtailed in the east by NE-SW trending right lateral strike slip faults, while in the west they flow into the Sulaiman Depression (Raza et al., 1990). From the Jurassic to the Late Cretaceous, the region that is now Khairpur High Range was in a basinal location. During the Lower Cretaceous, the depocenter was located to the east of the high, due by rapid subsidence.

During the Early Tertiary period, the Khairpur High experienced uplift due to wrench-driven forces, resulting in erosion of Upper Cretaceous Mughal Kot and Pub Formations on the high. The Khairpur High underwent normal faulting, trending northwest-southeast, possibly due to strike-slip movement along the western plate border. Following a Base Tertiary unconformity, Kanikot clastic deposits were laid down. Before this uplift, during the Jurassic to the Late Cretaceous, the Khairpur High was located in a basin. The depocenter of this basin was formed during the lower Cretaceous Age Tertiary unconformity. From the Lower Eocene to the Middle Eocene, the Khairpur High once again occupied a basinal position. The last uplift of the Khairpur High began during the Oligocene period and was the result of the continental collision between India and Eurasia at the western and northern basin boundaries. This uplift persisted until the late Cenozoic era.

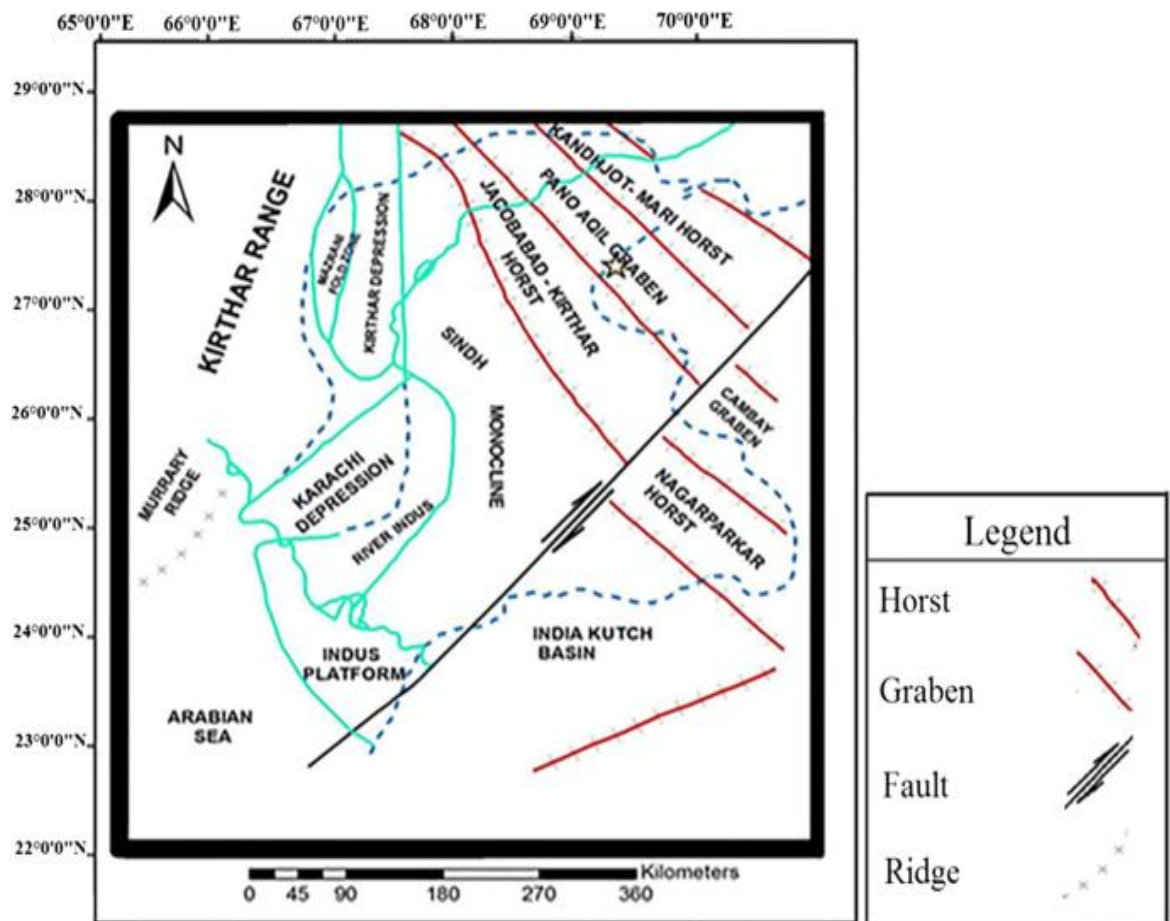


Figure 2.2. Generalized tectonic map of the study area and adjoining regions in the Central Indus Basin. Study area is located on PanoAqil Graben in between Mari-Kandhkot Horst and Jacobabad-Kirthar Horst.

2.3.2 Regions Structural Setting

Our study area is located in Block-20, which lies within the Central Indus Basin of Pakistan. The basin is bordered by heavily folded mountains on the east and west, namely the Indian Shield and the Axial Belt, respectively. The Khairpur High is a significant basement-induced structure that disrupts the Sindh Platform's westward dip. Beyond the Khairpur High, the Sindh Platform continues to slope westward and turns into a monotonous monocline that descends towards Karachi. The Pano Aqil Graben, which is a low-lying area, is where Block-20 is located. The eastern boundary of the Khairpur anticline is marked by outcrops of the Middle Eocene Habib Rahi Limestone, which has a gentle eastward dip that becomes a northeastern dip at Sukkur. The Ghazij shales of the middle to lower Eocene were discovered at Khairpur-2 and Kandra-1 wells, located on the crest of the anticline, beneath a layer of alluvial deposits on the western flank of the anticline. Eocene limestone outcrops are sparse in the southern portion of the block, but the underlying geology is unique. A diagram depicting the primary structural elements of the Central Indus Basin is presented in Figure 2.1.

2.3.3 Stratigraphy of the Central Indus Basin

The stratigraphy of the Central Indus Basin in Pakistan is intricate and can be categorized into various formations. One of these formations is the Lower Goru Formation, which is composed of both sandstone and shale and is part of the Lower Indus Basin. The Ranikot Formation, which consists mainly of sandstone, marks the beginning of the Paleocene epoch. The Sui Main Limestone, which is composed of limestone and marl, is a significant formation that marks the beginning of the Eocene epoch. The Pab Formation, which is primarily composed of sandstone, is the next formation, followed by the Lower Nari Formation, which is primarily composed of shale and siltstone. The Ghazij Formation, which is composed of shale, sandstone, and limestone, marks the beginning of the Oligocene epoch. The Kirthar Formation, which is primarily composed of sandstone and shale, marks the end of the Oligocene epoch and the beginning of the Miocene epoch. These formations have been further subdivided into members and units based on lithological and stratigraphic characteristics.

Age		Form	Member	
PLIOCENE	Upper	Swalik Group	SWALIK	
	OLIGOCENE		NARI	NARI
EOCENE	Middle Upper	Kirthar	ORAZINDA	
			PIPKOH	
			SIRKI	
			HABIB RAHI	
	Lower	Leki	GHAZU SHALE	
			SUI UPPER	
			SUI SHALE	
			SUI MAIN	
PALAEOCENE		Rerikot	DUNGHAN	
			UPPER RANIKOT	
			LOWER RANIKOT	
CRETACEOUS	Upper	Upper	Pab	PAB
			Mughal kot	Mughal Kot
	Middle	Parh	PARH	
	Lower	GORU	UPPER GURU	
			LOWER	GS30
				GS20
	GS10			
	Sembar	SEMBAR		
JURASSIC	MIDDLE	CHILTAN	CHILTAN	

Figure 2.3. Generalized stratigraphy of Central Indus Basin (Khan et al., 2017)

2.3.3.1 Sembar Formation

The Sembar Formation is a geological formation found in the Central Indus Basin of Pakistan. It was deposited during the early Eocene epoch and consists of sandstone and shale layers with occasional limestone interbeds. The formation has a maximum thickness of around 1000 meters and is an important hydrocarbon reservoir in the region, particularly in the southern parts of the basin. The formation was named after the Sembar River, which flows through the type locality in Balochistan, Pakistan.

2.3.3.2 Goru Formation

The Indus Basin is home to the Goru Formation, which ranges in age from the Aptian to the Coniacian. While the Sembar Formation's lower portion is made up of sandstone interbedded with shale and siltstone in eastward subsurface well data, (Williams, 1959; Fatmi, 1977). Based on sedimentary facies records, the Goru Formation is divided into the Lower Goru and Upper Goru Formations. Aged in the Lower Cretaceous, the Goru Formation (Aptian - Albian) 250 to 100 metre thick , Environment: Lower coast facies to deltaic with a barrier bar. The lateral extension of the lithostratigraphic section reflects the Indian Plate's continuous subsidence, which is accompanied by frequent transgressions and regressions or rises and falls in sea level. In the western and eastern halves of the study area, respectively, argillaceous limestone and sandstone with alternating shale beds make up the Lower Goru sedimentary facies.

The Southern Indus Basin has extensively developed these siliciclastic deposits (Ahmad et al., 1996; Ahmed et al., 2004 & 2012). Upper Goru Formation's age is Upper Cretaceous (Cenomanian – Coniacian) Based on fossil evidence, Williams describes the era (1959). Shale and argillaceous limestone make up the 500–400 metre thick lithology of the Upper Goru. a shallow to deep marine environment. The central and southern Indus Basin's upper Goru Formation is made up of shales interbedded with siltstones and claystone, while the western portion is made up of interbedded argillaceous limestone shale. But in the Punjab Platform region, which is located in the eastern part of the research area, it thins out and comes to an end. Sea levels rose to the east during the Cenomanian to Coniacian period, which is represented by this change in lithostratigraphy.

2.3.3.3 Parh Formation

The Parh Formation's lithology is dominated by limestone. shallow waters in the ocean It has been discovered in several wells in the Central Indus Basin. Its thickness is thinner in the eastern part of the study area. Fort Munro and Mughal Kot were built: Strong limestone makes up the 1600 to 500 metre thick Fort Munro Formation, which dates back to the Upper Cretaceous (Early Campanian to Early Maastrichtian). shallow waters in the ocean. However, the thickness decreases as you move east. In shallow water, the majority of the Mughal Kot Formation was created (Shahid et al., 2016). The thick bedded limestone of the Fort Munro Formation is uniformly layered over the Mughal Kot Formation in the Sulaiman fold belt (Williams, 1959; Fatmi, 1977). Its thickness varies from 50 to 250 metres in the Central Indus Basin. The eastern part of the research region has a thinner layer.

2.3.3.4 Pab Sandstone

The Pab Sandstone is a formation in the Central Indus Basin of Pakistan, which is composed of sandstones, siltstones, and shale. It is of Early Cretaceous age and was deposited in a fluvial-deltaic environment. The Pab Sandstone is an important hydrocarbon reservoir in the region, hosting several significant oil and gas fields such as Miano, Kadanwari, and Zarghun South. It is characterized by good porosity and permeability properties, making it an excellent target for exploration and production activities. The Pab Sandstone is also known for its distinctive red color, which is due to the presence of iron oxide minerals in the sediment. The Pab Formation is mostly made up of sandstone, with a little bit of shale and mudstone (Shahid et al., 2016; Khan, 1999; Kadri, 1995). Fort Munro Formation is lying on top of it. However, in some places it does so erratically and lies on top of the Mughal Kot Formation (Shahid et. al., 2016).

2.3.3.5 Kirthar Formation:

Kirthar has four separate members: Le. Drazinda, Pirkoh, Sirki, and Habib Rahi (Vrendenburg 1908).

2.3.3.6 Drazinda Member:

Eocene is the age of Drazinda. A change in lithology from sandstone, clay, and conglomerate to claystone and limestone defined the upper border of the Drazinda member.

2.3.3.7 Pirkoh Member:

Pirkoh's members are Eocene in age. A change from marl to limestone in the lithology defined the top border of the Pirkoh member. Limestone, ranging in colour from pale yellowish grey to pale yellowish green, makes up lithology (Vredenburg, 1908).

2.3.3.8 Sirki Member:

Age of a Sirki Member is Eocene. A change in lithology from limestone to claystone determined the upper border of the Sirki component. It is dark bluish green in Claystone (Williams, 1959).

2.3.3.9 Habib Rahi Member:

A Habib Rahi member is an Eocene. Limestone is a white to light yellowish grey stone with a blocky texture that is firm to fairly hard. Claystone is subplaty, amorphous, and mildly calcareous in some sections. Its colour ranges from medium to dark greenish grey (Vredenburg, 1908).

2.3.3.10 Ghazij Member:

Age-wise, a Ghazij member is Eocene. The change in lithology from limestone to shale defines the upper border of the Ghari component. The tone of shale is light to medium grey (Williams, 1959).

2.3.3.11 Sui Main Limestone:

Sui Main Limestone member is Eocene in age. The upper limit of the Sui Main limestone component is defined by a transition in lithology from shale to limestone. Limestone has a light-yellow grey tint and contains traces of crystalline calcite as well as uncommon traces of chert (Williams, 1959).

2.3.3.12 Ranikot Formation:

Ranikot Formation is Paleocene in age. Marl has a light to medium grey hue, is soft to firm, amorphous, sub blocky, and locally grades to calcareous claystone.

2.4 Petroleum System

2.4.1 Source Rocks

The Central Indus Basin is known to contain several source rocks that have generated significant amounts of hydrocarbons. The most important source rocks in the Central Indus Basin are found in the Lower Goru and Sembar formations, which were deposited during the Cretaceous Period, approximately 65 to 145 million years ago.

The Lower Goru Formation contains organic-rich shales that have undergone thermal maturation to generate hydrocarbons, such as oil and gas. The shales in the Lower Goru Formation are known to be the source of most of the oil and gas reserves in the Central Indus Basin. The Lower Goru Formation is composed of sandstone, shale, and limestone, and is estimated to be between 200 to 350 meters thick.

The Sembar Formation is another important source rock in the Central Indus Basin, and it is located above the Lower Goru Formation. It is also composed of shale, sandstone, and limestone, and is estimated to be between 100 to 250 meters thick. The organic-rich shales in the Sembar Formation have also undergone thermal maturation to generate hydrocarbons. Other formations in the Central Indus Basin, such as the Ranikot and Pab formations, also contain organic-rich shales that may act as potential source rocks for hydrocarbons. These formations are located above the Sembar Formation and are also composed of sandstone, shale, and limestone. Overall, the Central Indus Basin is an important hydrocarbon province, and the source rocks within it have contributed significantly to the oil and gas reserves in the region.

2.4.2 Reservoir Rocks

The Central Indus Basin is known to contain several reservoir rocks that have trapped and stored significant amounts of hydrocarbons. The most important reservoir rocks in the Central Indus Basin are sandstone formations, which were deposited during the Cretaceous Period, approximately 65 to 145 million years ago. The most important sandstone reservoir rocks in the Central Indus Basin are found in the Lower Goru and Upper Sand formations. The Lower Goru Formation is composed of sandstone, shale, and limestone, and is estimated to be between 200 to 350 meters thick. It is an important hydrocarbon reservoir in Pakistan, and a number of oil and gas fields have been discovered within it.

The Upper Sand Formation is also an important sandstone reservoir rock in the Central Indus Basin. It is composed of sandstone and shale, and is estimated to be between 150 to 200 meters thick. It is an important hydrocarbon reservoir in Pakistan, and a number of oil and gas fields have been discovered within it as well. Other sandstone formations in the Central Indus Basin, such as the Pab, Chiltan, and Hangu formations, also act as potential reservoir rocks for hydrocarbons. The confirmed hydrocarbon reserves in the region are found in sandstone formations that were deposited during the Cretaceous Period, specifically in the bottom portion of the Lower Goru Formation, as well as in sandstone formations from the Paleocene Ranikot Formation and the Eocene Sui Main Limestone. These formations contain significant hydrocarbon reserves that have been confirmed through exploration and production activities in the region (Iqbal et al., 2011).

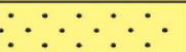
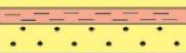



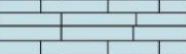
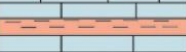
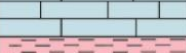

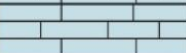


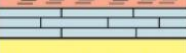
2.4.3 Seal Rocks

Shales interbedded with sandstone formations act as effective seals in the Central Indus Basin, covering the hydrocarbon reservoirs. These shale strata, varying in thickness, function as efficient seals in areas of hydrocarbon production. Impermeable seals above truncation traps and faults may also be beneficial. In the Lower Indus Basin, the Upper Goru shale and interbedded shales of Sui Main Limestone are known to operate as seals (Iqbal et al., 2011).

2.4.4 Traps

The Central Indus Basin of Pakistan contains various types of traps that can hold hydrocarbons. These traps include anticlinal traps, fault traps, stratigraphic traps, and combination traps. Anticlinal traps are created by folds in the rock layers that form domes or arches. Fault traps are formed when there is movement along a fault line, causing a displacement of the rock layers and creating a trap for hydrocarbons. Stratigraphic traps are formed by variations in the rock layers, such as pinch-outs or truncations, which create barriers to the flow of hydrocarbons. Combination traps are formed by a combination of these different types of traps. These traps can hold hydrocarbons in sandstone reservoirs such as Lower Goru Formation, Ranikot Formation, and Sui Main Limestone. Proper identification and characterization of these traps are essential for successful hydrocarbon exploration and production in the Central

Indus Basin. The area's horst and graben features serve as excellent hydrocarbon traps. (Quadri and Shuaib, 1986).

Age	Formation	Lithology	Depth (m)
Miocene	Siwalik Group		0
			
Eocene	Drazinda Fm		500
	Pirkoh Fm		567
	Sirki Fm		671
	Habib Rahi Fm		740
	Ghazij Fm		864
	Sui Main Limestone		1483
Paleocene	Ranikot Fm		1676
Cretaceous	Upper Goru Fm		1899
	Lower Goru Fm	  	2226

Legends

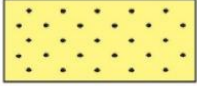

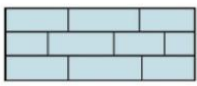
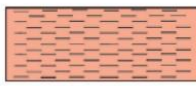
	Sandstone		Shale
	Limestone		Clay

Figure 2.4. Study Area stratigraphy Ahmed et al 1990.

CHAPTER 3

SEISMIC DATA INTERPRETATION

3.1 Introduction

In order to understand the subsurface geology or get the better idea of how the things are placed in subsurface we need to get the better or more appropriate image of the subsurface. To get the desired output or desired results of subsurface a proper work flow is required through the process of seismic acquisition, seismic interpretation and seismic processing. These are also known as the methodologies that are being used in the research process. These methodologies are more or less same for these type of data sets. The interpretation of reflection data involves expressing it in geological terms. When fully implemented, it necessitates the integration of all relevant geological and geophysical data into a more comprehensive and trustworthy image than any source is likely to provide alone.

This integration would be most efficiently performed if a single individual was extremely knowledgeable in both geophysics and geology. This is crucial for accurate estimate of the geometry and depth of the target horizons or bed rock. Seismic reflection surveys are primarily used to expose the subsurface structures and stratigraphy as clearly as feasible. Seismic reflection's geological significances are merely a marker for various borders where the acoustic impedance changes. Different geological features and stratigraphic connections are connected to these observed contrasts. There are two primary methods for interpreting seismic section, structural and stratigraphic analysis.

Structural interpretation is the process of analyzing geological data, such as seismic reflection data, well logs, and geological maps, in order to create a three-dimensional model of the subsurface structure. This involves identifying and mapping the various geological features, such as faults, folds, and stratigraphic horizons, and understanding how they relate to each other. Structural interpretation is used in a variety of industries, including oil and gas exploration, mining, and civil engineering, to help guide exploration and development activities.

3.2 Seismic Data

The 2D seismic data comprises of 1500-line kilometer acquired in three vintages, in and out of Miano area. We selected 8 lines out of the total lines for our

thesis purpose on which we perform the seismic interpretation. These lines also comprise of the well Miano-02 which has the total depth of 3852m.

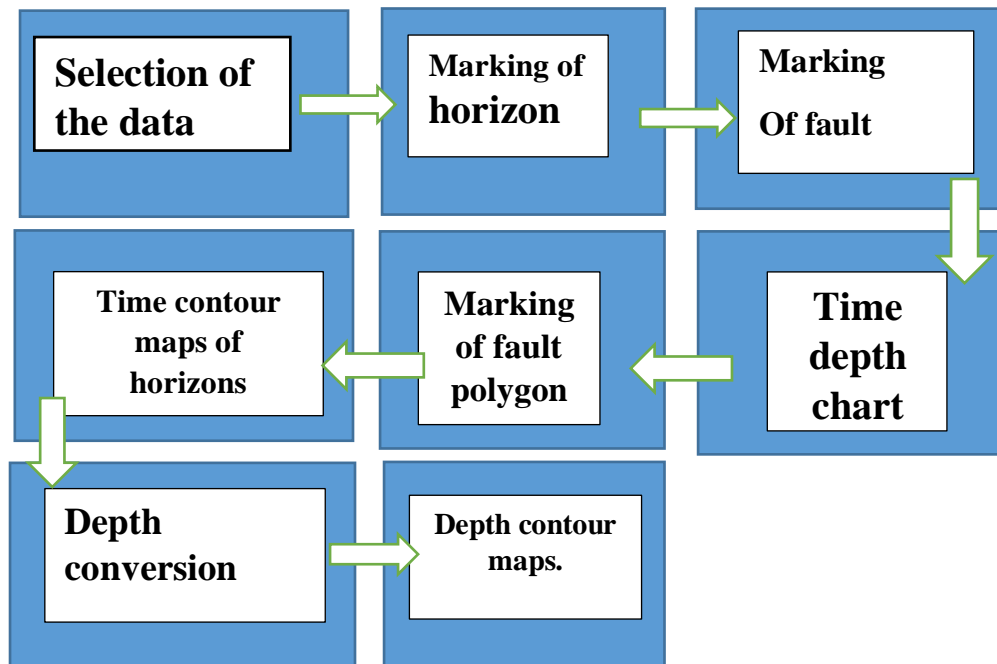


Figure 3.1. Seismic Interpretation Workflow adopted for the study.

3.3 Base Map

In this study, the Base Map serves as a visual representation of the lease or concession boundaries and seismic survey points, providing information such as latitude and longitude or UTM grid references. Geophysicists use shot points maps to display the interpretations of seismic data, indicating the orientations of seismic lines and specific points where seismic data was collected. The Base Map utilized in this research comprises a total of eight lines, of which six are dip lines (SP-2092-111, SP-2092-113, SP-2092-115, SP-2092-117, SP-2092-119, and SP-2092-121) that extend from west to east, while the other two are strike lines (SP-2092-114 and SP-2092-116) that extend from north to south. The North arrow denotes the direction of the lines, and the location of well Miao-02 establishes SP-2092-113 as the control line.

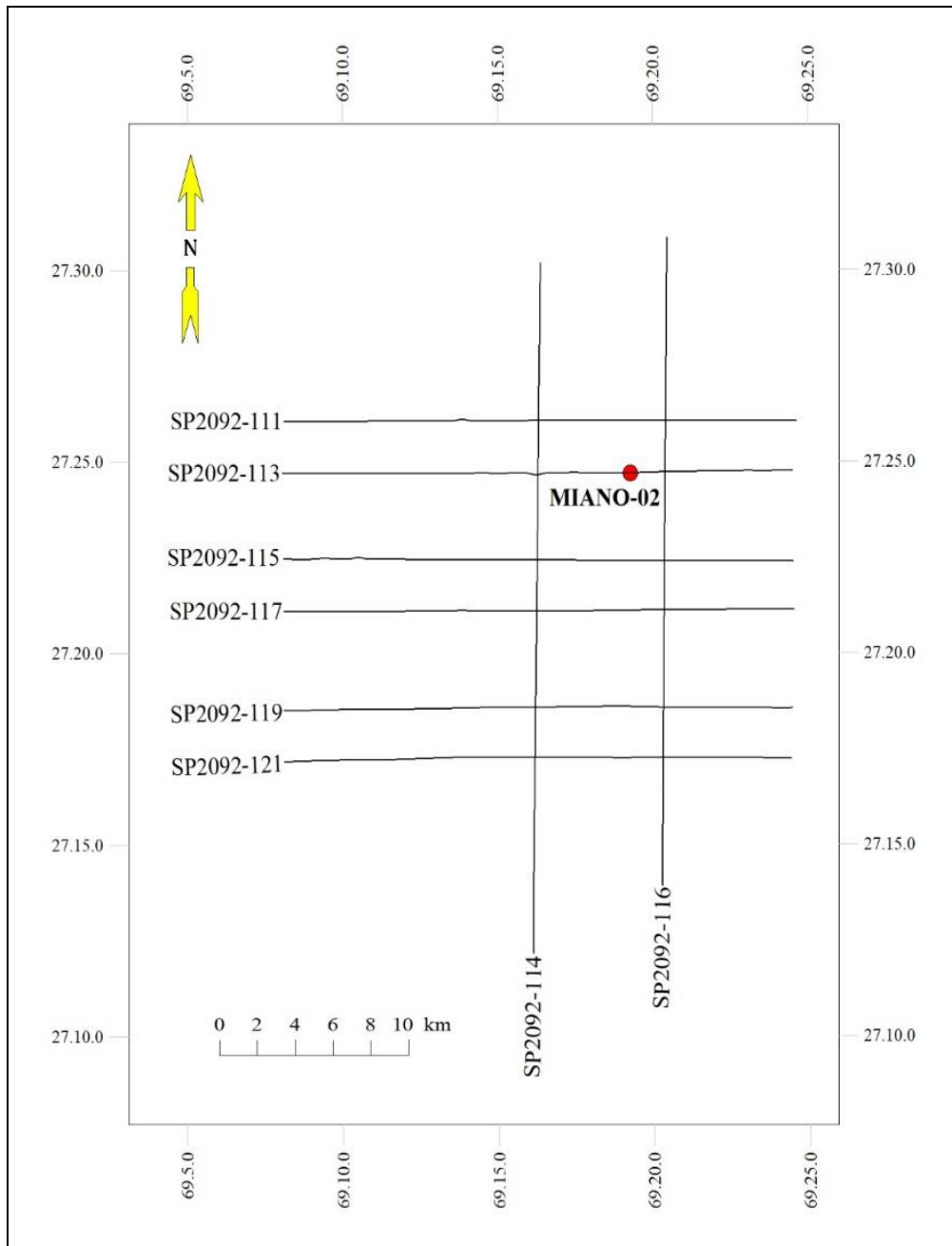


Figure 3.2. Base Map of Miano area showing location of seismic lines and Miano-02 well.

3.4 Time Depth Chart

Time depth chart is prepared to perform the well to seismic tie as the seismic data is in time domain and well data is recorded in depth domain. The velocity window available on the seismic section at the well location is taken from which depth is calculated using the time and velocity information. Using this Time depth relation, prominent reflectors are marked on the control line, which are then further transferred to other seismic lines using jump and loop tie method.

Table 3.1. Time Depth chart prepared from the velocity window given at the seismic line.

Time (sec)	Vrms(m/s)	Depth(m)
425	1557	330.8625
728	1859	676.676
1081	2014	1088.567
1375	2383	1638.313
1974	2689	2654.043
2269	3097	3513.547
2667	3561	4748.594
3058	3688	5638.952
4000	4049	8098

3.5 Picking of Horizon

After marking the horizon on seismic line next step is to mark the fault marking along the surface. The horizon that is to be picked depend upon our area, its geological setting, depth of reservoir etc. our main zone of interest lies in the Lower Goru, Upper Goru and Habib Rahi as well. So that's why we marked these three horizons on our seismic section.

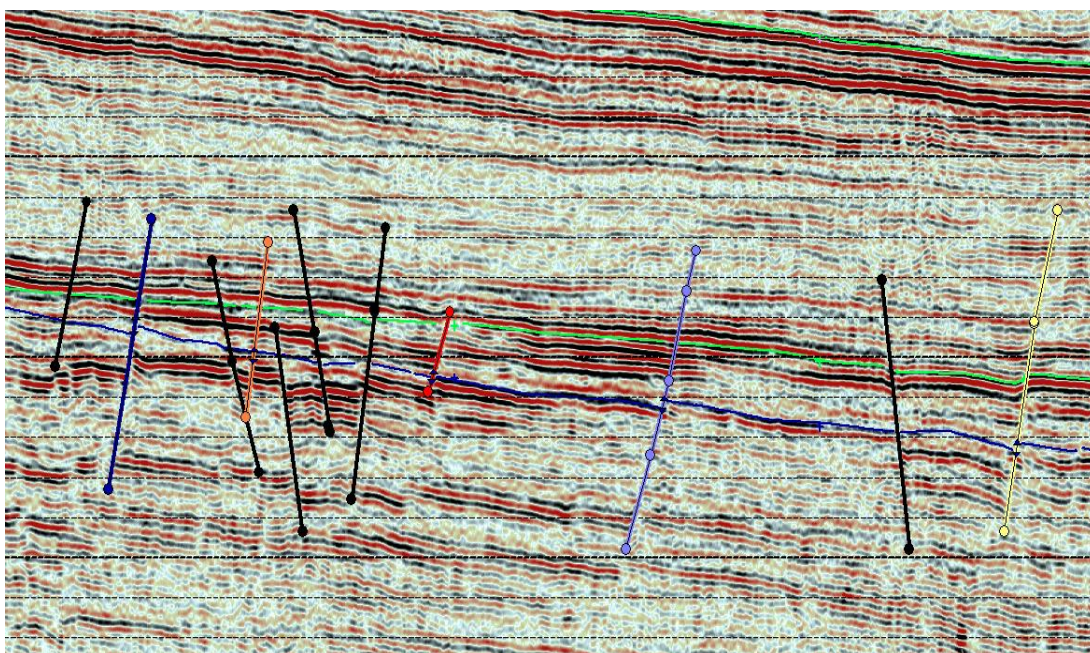


Figure 3.3. Horizon picking based on the time depth chart of the Miano area.

3.6 Fault Picking and Correlation

This area lies in the middle Indus basin of Pakistan which is extensional regime. So as we know that in the extensional regime normal faults are created. This area also shows the clear structural pattern i.e. horst and graben structure. And we can also observe the thickening of layers as we move downward. During fault picking in lower as well as upper Goru we encounter 5 major faults that cuts the dip lines shows some specific behavior. the major faults as shown in figure are mostly straight in nature. Comparing Lower Goru and Upper Goru with Habib Rahi, Habib Rahi is more stable in nature as it is present on shallow depth and less effected by tectonics. These faults are slightly tilted as we move downward. Next point is to correlate these faults on other lines, so in Gverse Software first we mark or name the fault and then pick the heave of the fault. That how the fault will correlate or match on the other line. Once all the faults on every line is picked, then the fault cut were applied so that these faults can be marked on the base map as well.

3.7 Interpretation of Seismic Lines

3.7.1 Interpretation of P2092-113

P2092-113 is a dip and control line oriented in EW direction covering a length of 3075 m/ 3 km. it's also our control line because well Miano-02 lies on VP 470. Five faults are identified on this seismic line, All major faults are dipping in NW direction Faults F1 and F2 are forming and horst and graben type structure.

3.7.2 Interpretation of P2092-111

P2092-111 is a dip, oriented in NW direction covering a length of 3075 m/ 3 km. numerous faults are identified on this seismic line, out of which five are major faults. Faults F1, F2, F3, F4 and F5 are dipping in NW direction forming normal faults. Horizons are dipping in EW direction. On the deeper part of the subsurface, number of faults can be observed because of intense tectonic as compared to the Habib Rahi which is present on shallow depth.

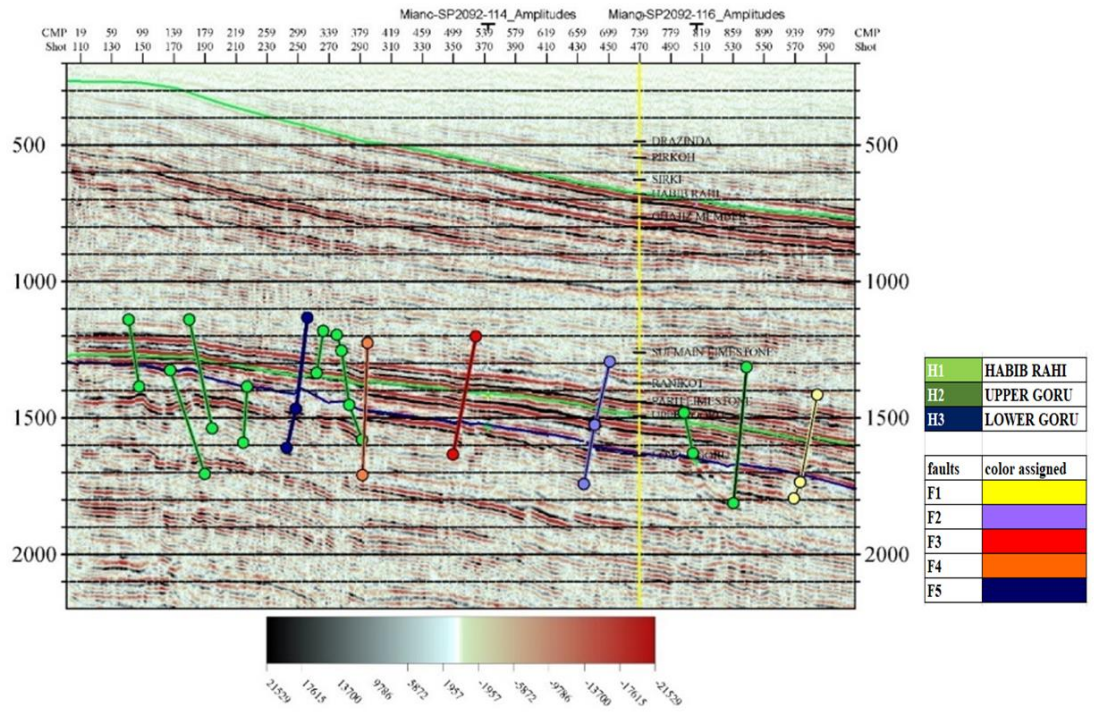


Figure 3.4. Interpreted seismic section of line P2092-113.

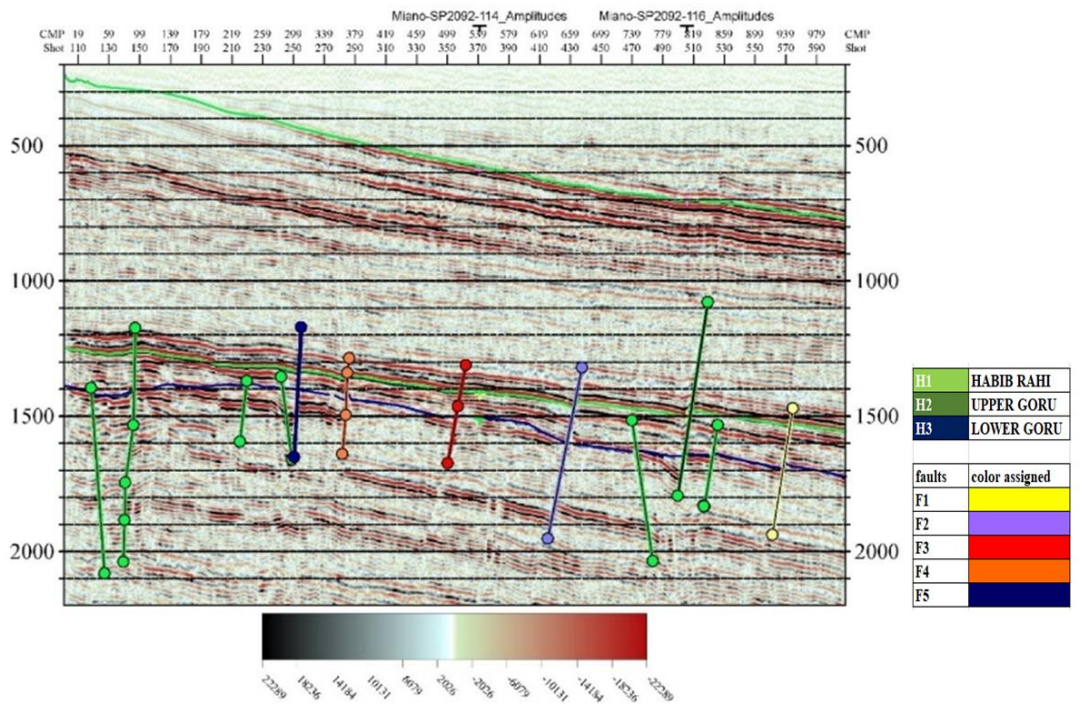


Figure 3.5. Interpreted seismic section of line P2092-111

3.7.3 Interpretation of P2092-115

P2092-115 is a dip line oriented in EW direction covering a length of 3075 m/3 km. three horst and graben structures are observed. Five faults are identified on this seismic. All the faults are trending in NW direction out of which F5 is more prominent. Faulting is more intense in this part.

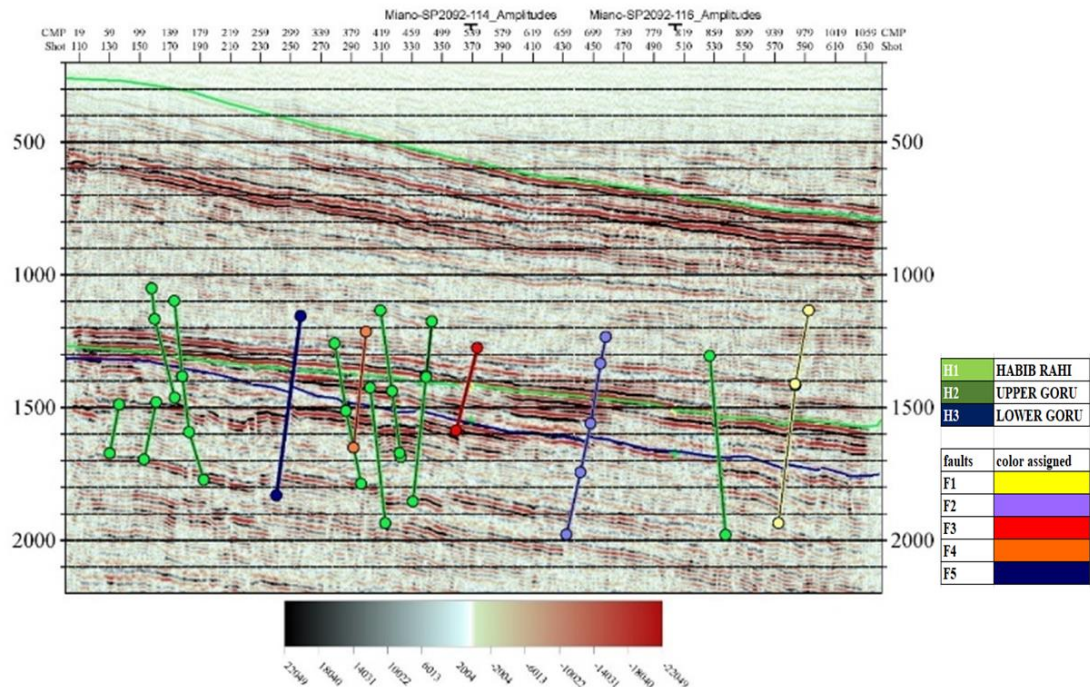


Figure 3.6. Interpreted seismic section of line P2092-115.

3.7.4 Interpretation of P2092-117

P2092-17 is a dip line oriented in EW direction covering a length of 3075 m/3 km. Seven horst and graben structures are observed. Five major faults are identified along with other minor faults on this seismic section. All the faults are trending in NW direction out of which F1, F3 and F5 is more prominent. As we are moving downward faulting is getting intense in this area.

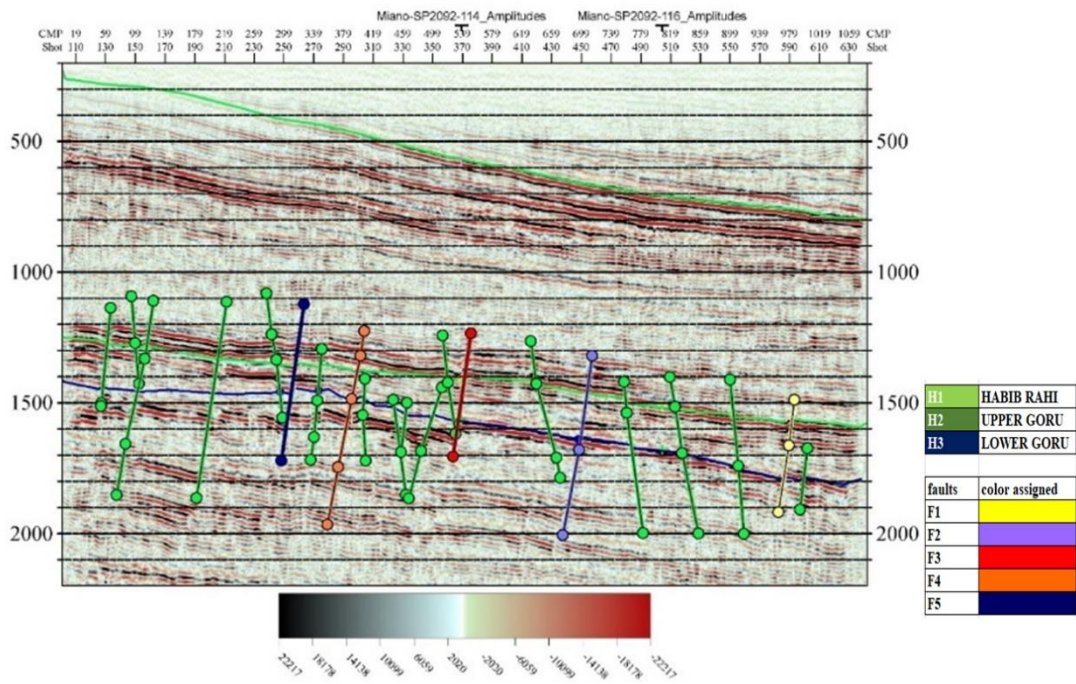


Figure 3.7. Interpreted seismic section of line P 2092-117

3.7.5 Interpretation of P2092-119

P2092-19 is a dip line oriented in EW direction covering a length of 3075 m/3 km. Horst and Graben structures are observed. Five major faults are identified along with other minor faults on this seismic section. All the faults are trending in NW direction out of which F1, F3 and F5 is more prominent. Because of intense faulting faults are reaching up to the Upper Goru.

3.7.6 Interpretation of P2092-121

P2092-121 is a dip line oriented in EW direction covering a length of 3075 m/3 km. Horst and Graben structures are observed. Five major faults are identified along with other minor faults on this seismic section. All the faults are trending in NW direction out of which F1, F3 and F5 is more prominent. Because of intense faulting faults are reaching up to the Upper Goru.

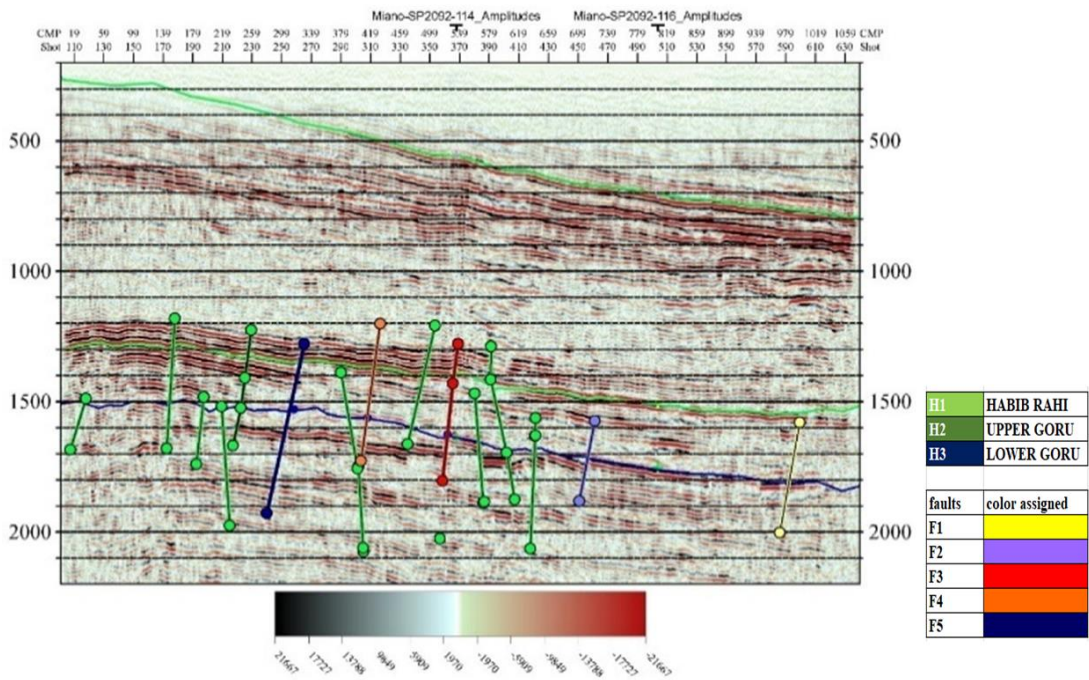


Figure 3.8. Interpreted seismic section of line P2092-119.

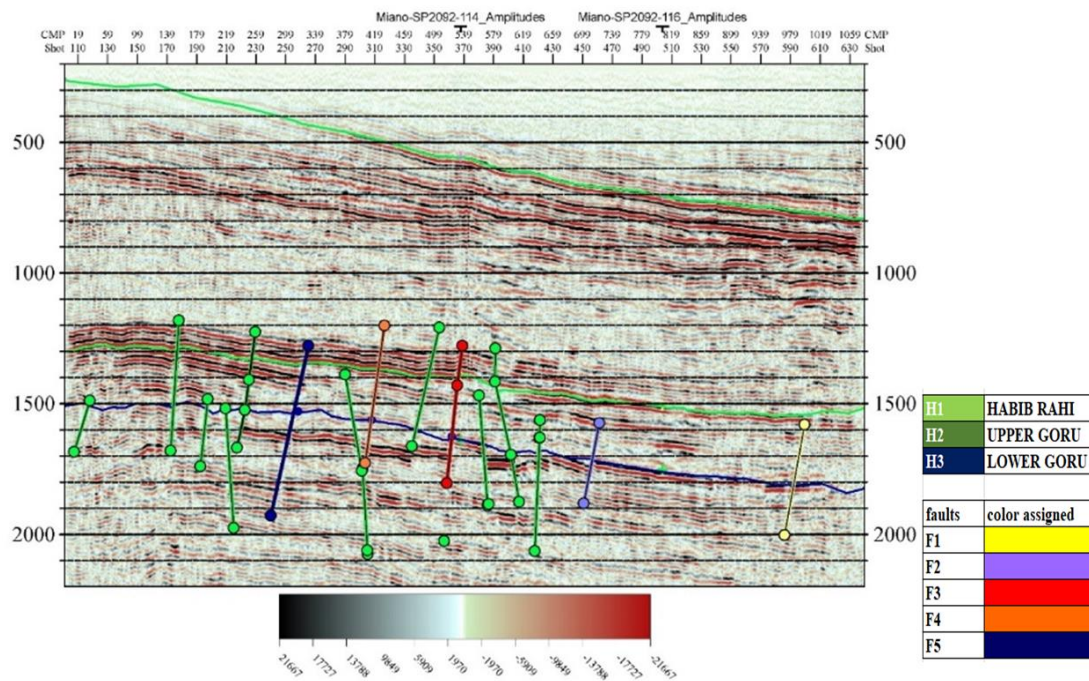


Figure 3.9. Interpreted seismic section of line P2092-121.

3.7.7 Interpretation of P2092-114

P2092-114 is a strike line oriented in NS direction covering a length of 3075 m/3 km. no major faults are observed on this line because of strike line are present in the direction to the faults. That's why more clear or smooth horizons are being observed.

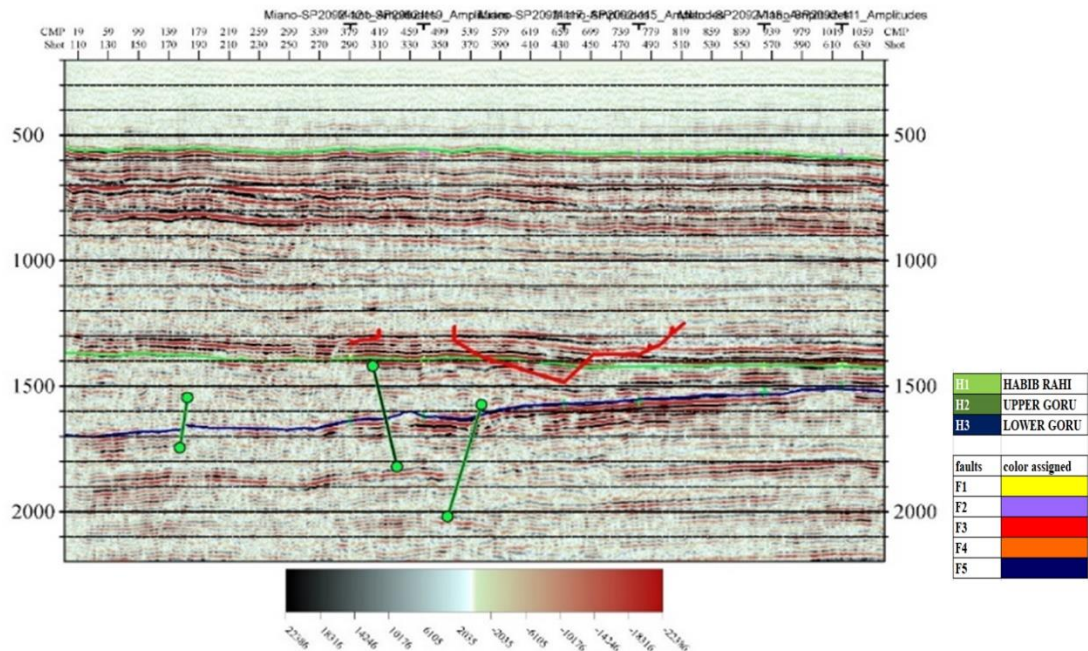


Figure 3.10. Interpreted seismic section of line P2092-114.

3.7.8 Interpretation of P2092-116

P2092-116 is a strike line oriented in NS direction covering a length of 3075 m/3 km. no major faults are observed on this line because of strike line are present in the direction to the faults. That's why more clear or smooth horizons are being observed.

3.8 Mapping

The Isomap layer is generated on Gverse Software of every horizon. Each map represents its own time of deposition. Then smoothing of contour interval was done on every isomap layer.

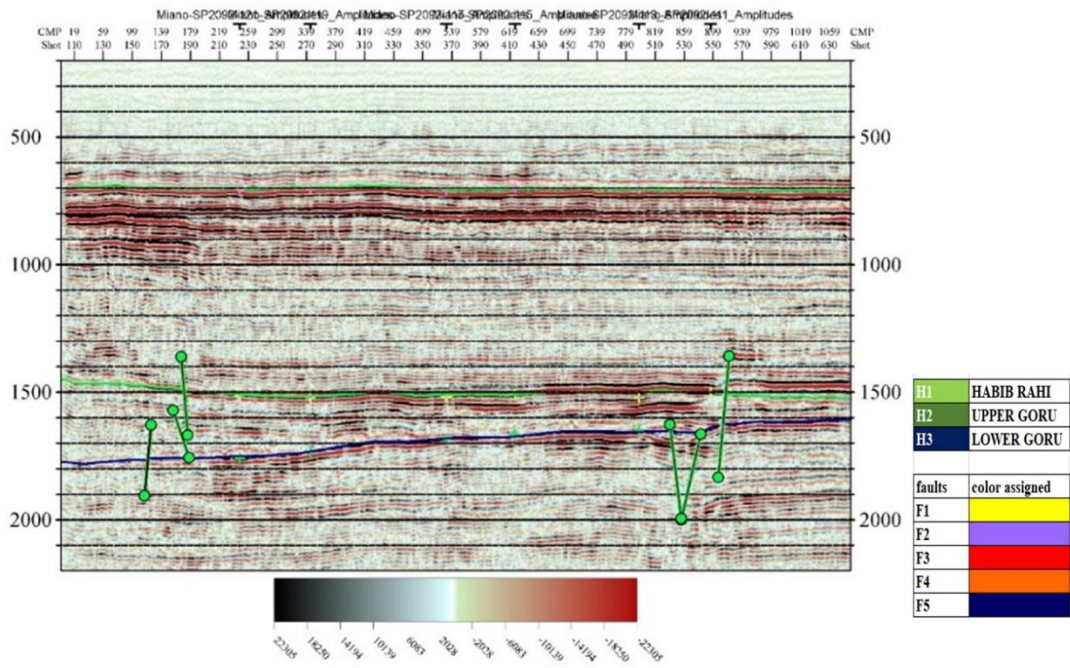


Figure 3.31. Interpreted seismic section of line P2092-116.

3.8.1 Time Contour Maps

For each of the three Horizons, a separate time contour map is being generated. In general, time sections show us how horizons are arranged in relation to time. These are used to calculate the two-way travel time, with different times chosen for various shot points. Tables are then prepared in Microsoft Excel, from which the data is exported and ran through the geverse software to produce time contours. Additionally, using the geverse software, time contour maps were created.

3.8.1.1 The Lower Goru Formation

Two-way time contour map demonstrates the diversity in the time values. shallower part is being represented by red whereas the deeper part is represented by color. The time variations can be seen while moving left to right. All the major faults polygon is marked on the contour map representing their directions in the area. Because of the compressional tectonic regime. The entire area contains horst and graben structures in which the hanging wall is moving downward with respect to footwall.

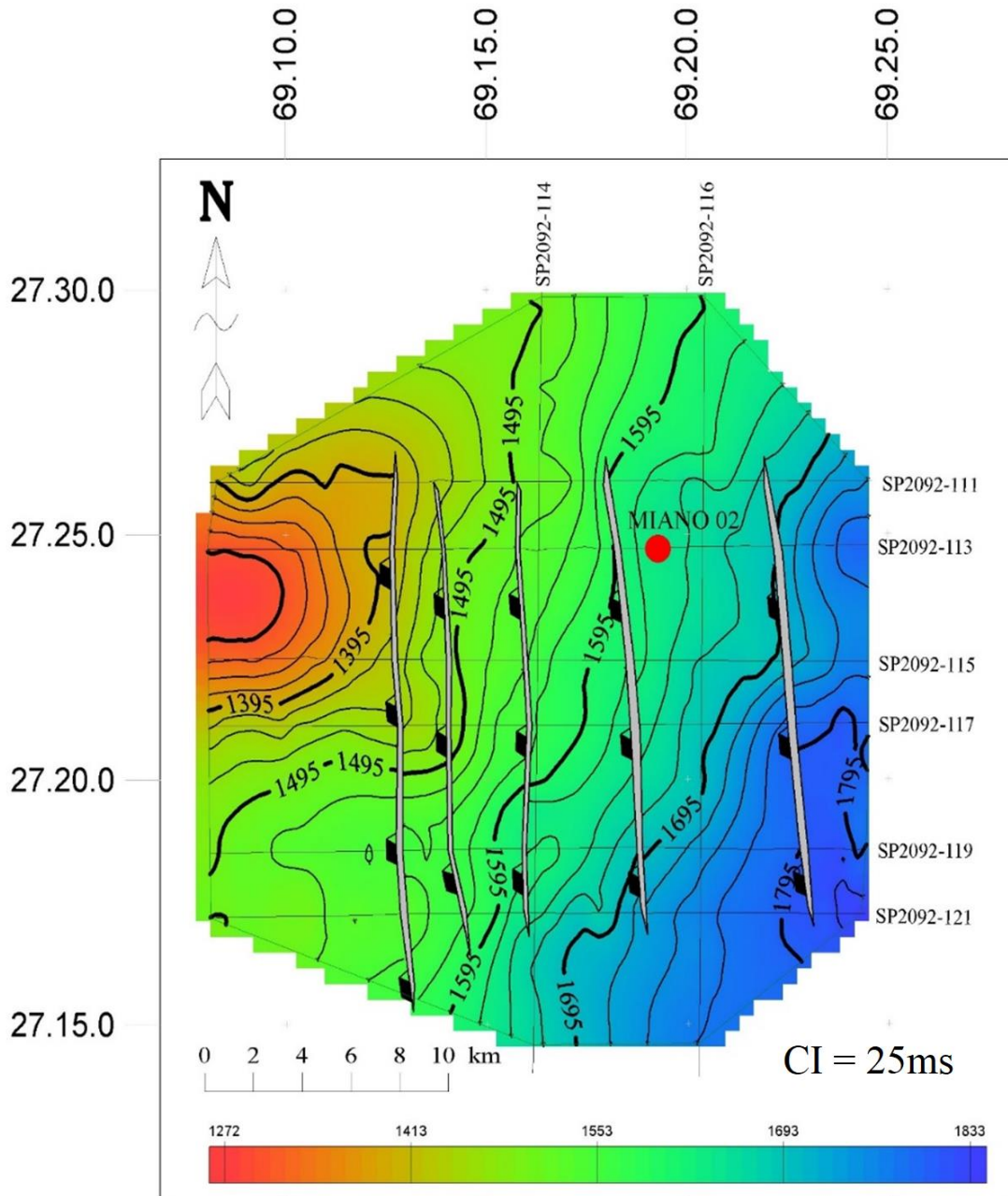


Figure 3.42. Time Contour Map of Lower Goru Formation in Miano field.

3.8.1.2 The Upper Goru Formation

Two-way time contour map demonstrates the variations in the time values in the study area. Upper Goru is present on shallower level as compare to the lower Goru because of which most of the contour map is filled with blue to green color. shallower part is being represented by blue whereas the deeper part is represented by red color. It has been observed that the deposited stratigraphic formation is getting shallower in EW direction. Time values are shown on the bold lines representing their elevation with respect to mean sea level. All the major fault's polygon is marked on the contour map

representing their directions in the area. Because of the compressional tectonic regime, the entire area contains horst and graben structures in which the hanging wall is moving downward with respect to footwall.

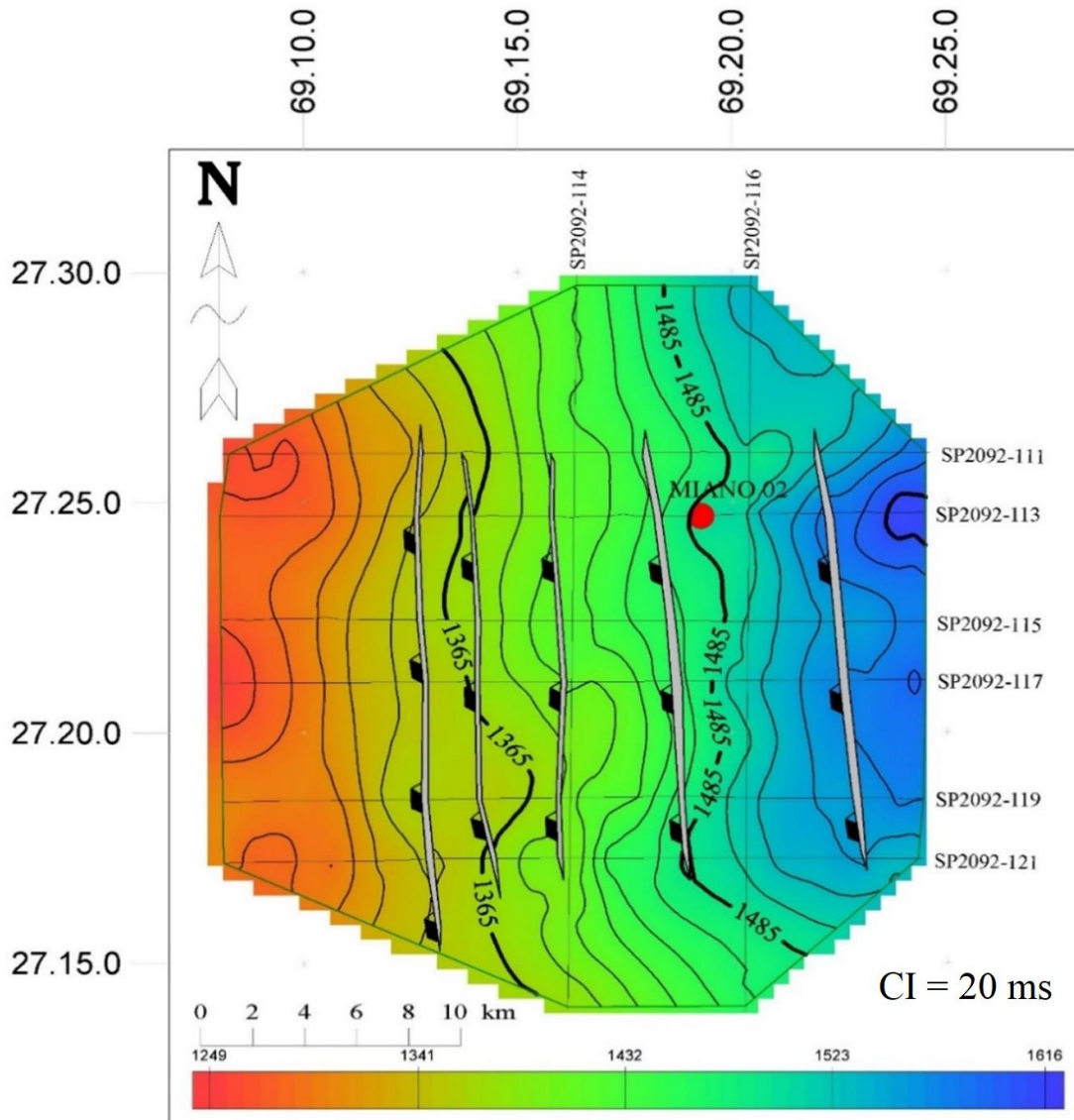


Figure 3.13 Time Contour Map of Upper Goru Formation in Miano field.

3.8.1.3 Habib Rahi Time Contour

The Habib Rahi Formation's two-way time contour map demonstrates the variations in the time values in the study area. Habib is present on shallowest level as compare to the lower Goru and Upper Goru because of which most of the contour map is filled with blue to green color. shallower part is being represented by blue whereas the deeper part is represented by red color. It has been observed that the deposited

stratigraphic formation is getting shallower in EW direction. Time values are shown on the bold lines representing their elevation with respect to mean sea level. No faults are observed along Habib Rahi formation because of its presence on shallower level and the contour are also showing very less to negligible changes along the area.

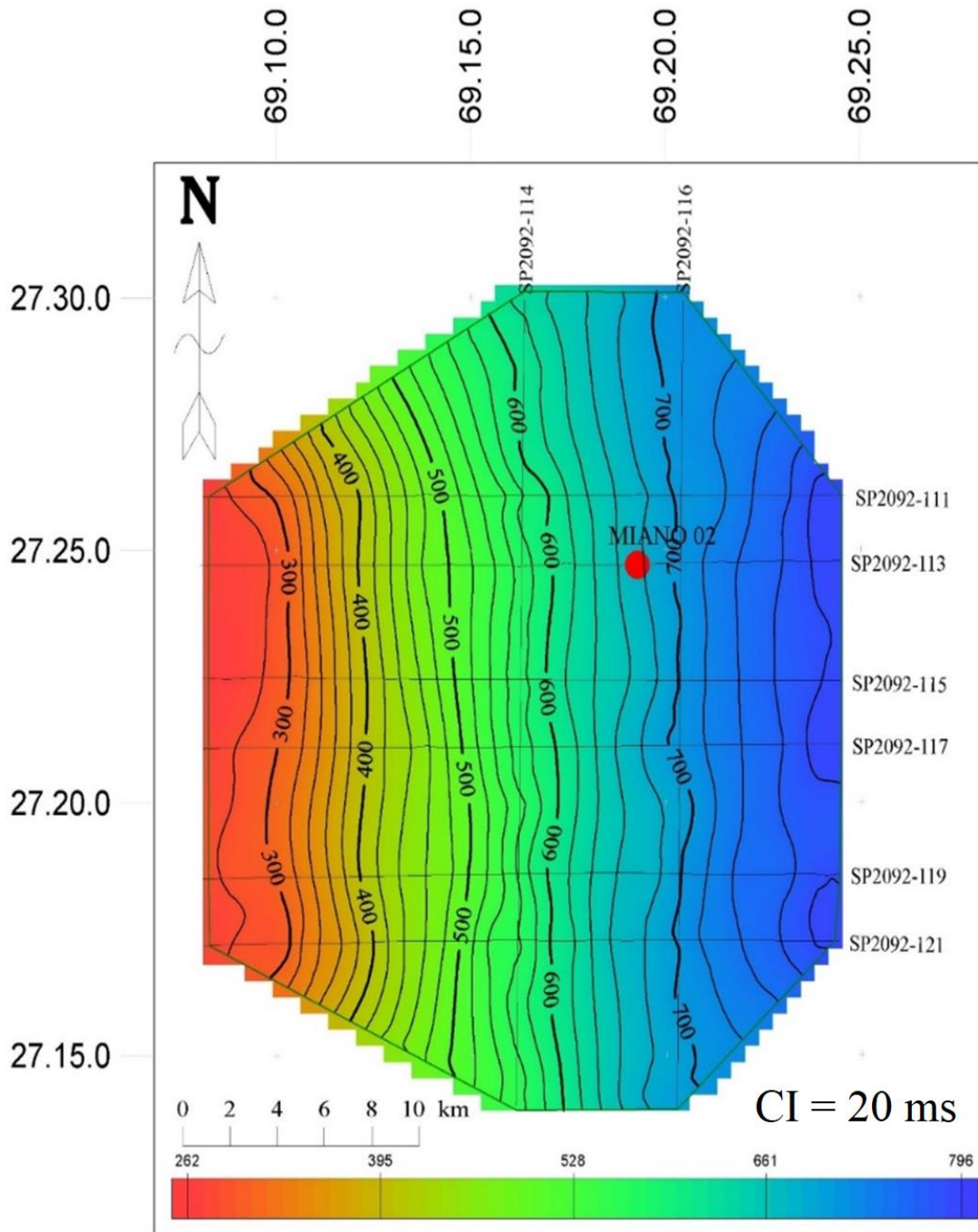


Figure 3.54. Time Contour Map of Habib Rahi Formation in Miano field.

3.8.2 Depth Contour Maps

The configuration of reflectors can be determined by the depth section, which works similarly to the time section. To calculate the depth of specific reflectors in the seismic section, the following formula is employed:

$$S = (V * T) / 2$$

where

S=Depth

V = velocity

T=The reflector's two-way time, as read from the seismic portion.

The software can be used to create the depth contour maps manually as well. For imaging of subsurface geological structures and trends, time and depth structure maps are created. Keep in mind that the time and depth maps show a similar subsurface arrangement. We can calculate the top of the horizons for which the depth map was created by looking at it. Horst and Graben structure with extensional tectonics is obvious from the time and depth maps. The reflector's two-way time, as read from the seismic portion. Steps for Calculating depth. For imaging of subsurface geological structures and trends, time and depth structure maps are created. Keep in mind that the time and depth maps show a similar subsurface arrangement. We can calculate the top of the horizons for which the depth map was created by looking at it. Value of Time and Depth was given only on Well Point where as we only have Value of Time (from seismic section). For finding the Velocity first we will add the value of depth of the targeted horizon and time from Seismic section and then multiply the resultant value with the 2000. Reason for multiplying it with 2000 was that it is a Two-Way Travel Time and time is given in Micro seconds. The resultant velocity is then multiplied by the time of the well which is further divided by 2000 to get the value of depth at every point.

3.8.2.1 Depth variation map of lower Goru:

The depth map shows variations in elevation along the Lower Goru horizon in the study area. The shallow part in the western region is depicted in blue, while the deeper part in the eastern region is depicted in red. The majority of the area on the depth map is filled with green color, indicating that the seismic data only covers the central

flat region of the area. The map also highlights the faults in the area, which dip in an East-West direction. The closely spaced contour lines on the map represent steep dips.

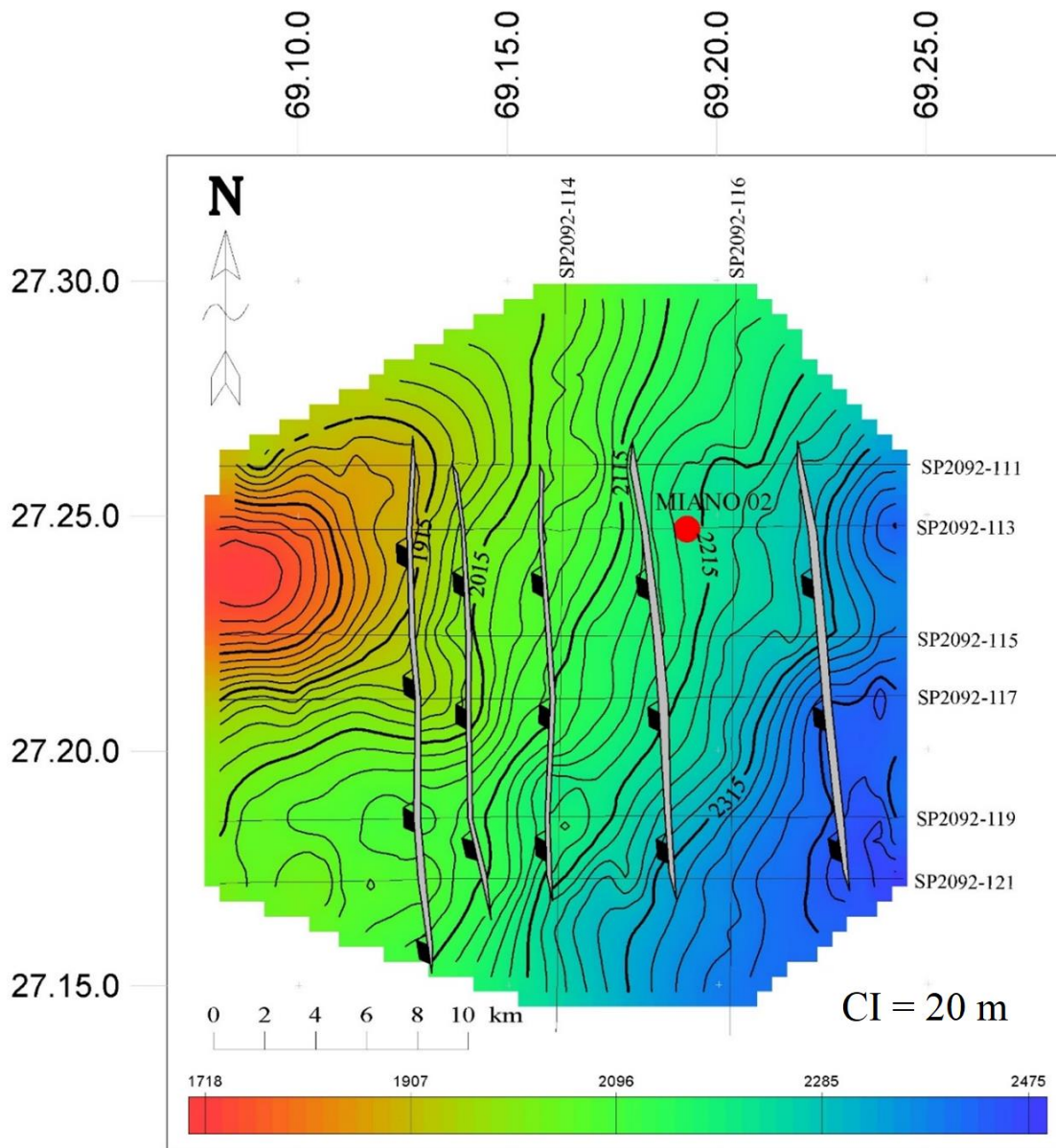


Figure 3.65. Depth Contour Map of Lower Goru Formation in Miano field.

3.8.2.2 Depth variation map of Upper Goru

Representing difference in elevation at different point along the marked Upper Goru. This map representing that the Upper Goru is present on shallower level because of which we can see very less reddish area. Blue color representing the shallow part in the western part of the study area and red color shows the deeper part in eastern side of the study area. Most of the area in depth map is represented by green and blue color fills representing the shallower part of the area. All of the faults are marked on the depth

map dipping in East-West direction. Closely placed contour lines are in the map representing the elevated part in the area.

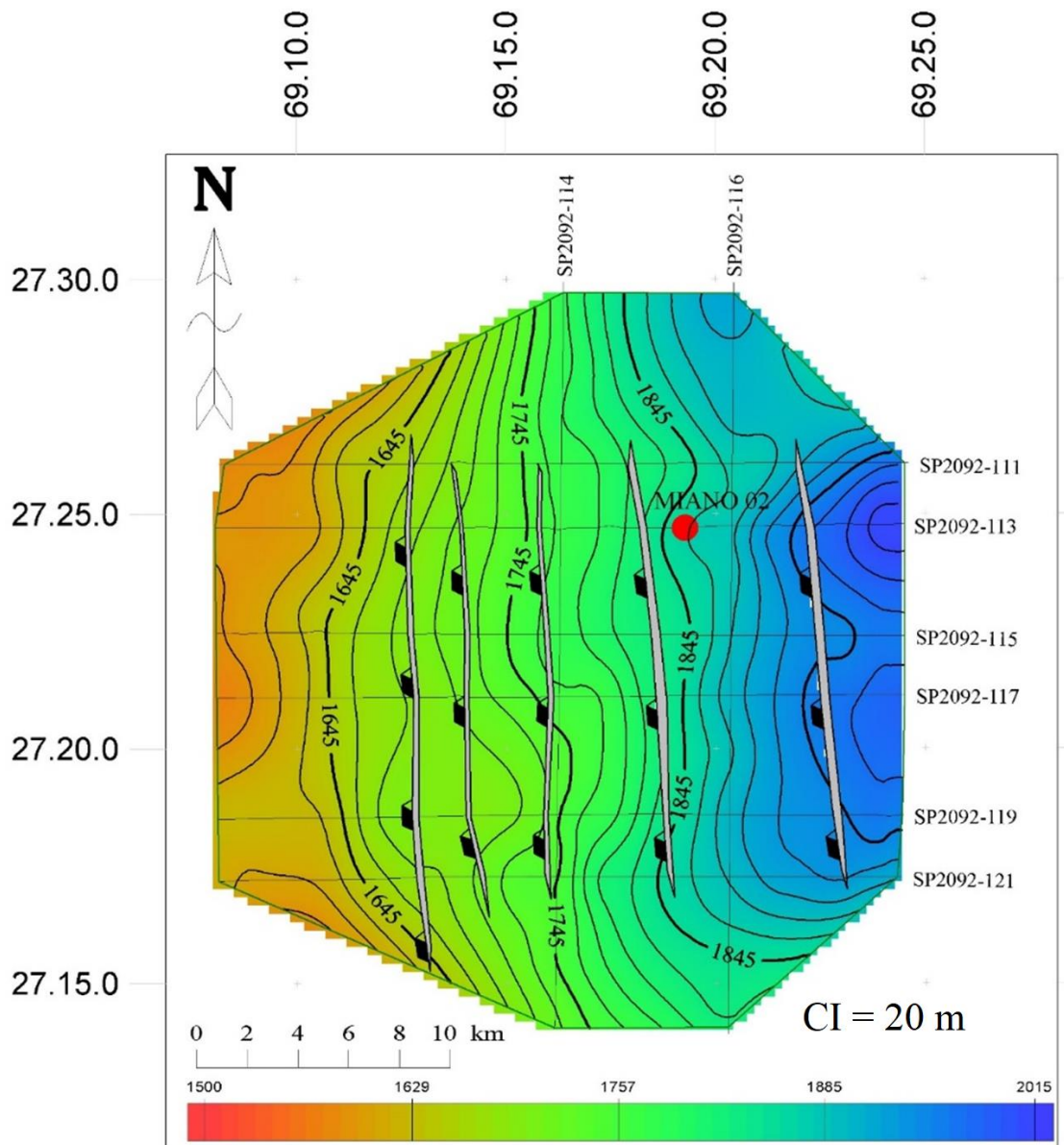


Figure 3.76. Depth Contour Map of Upper Goru Formation in Miano field.

3.8.2.3 Habib Rahi Depth Contour:

Blue color representing the shallow part in the western part of the study area and red color shows the deeper part in eastern side of the study area. Most of the area in depth map is represented by green and blue color fills representing the shallowest part of the area among all the three horizons. Faults are not marked on this map because faults didn't reach up to this level. As a very strong tectonic force is required to disturb

any lithology up to this level. Closely placed contour lines are in the map representing the elevated part in the area. Depth variation map of Habib Rahi representing difference in elevation at different point.

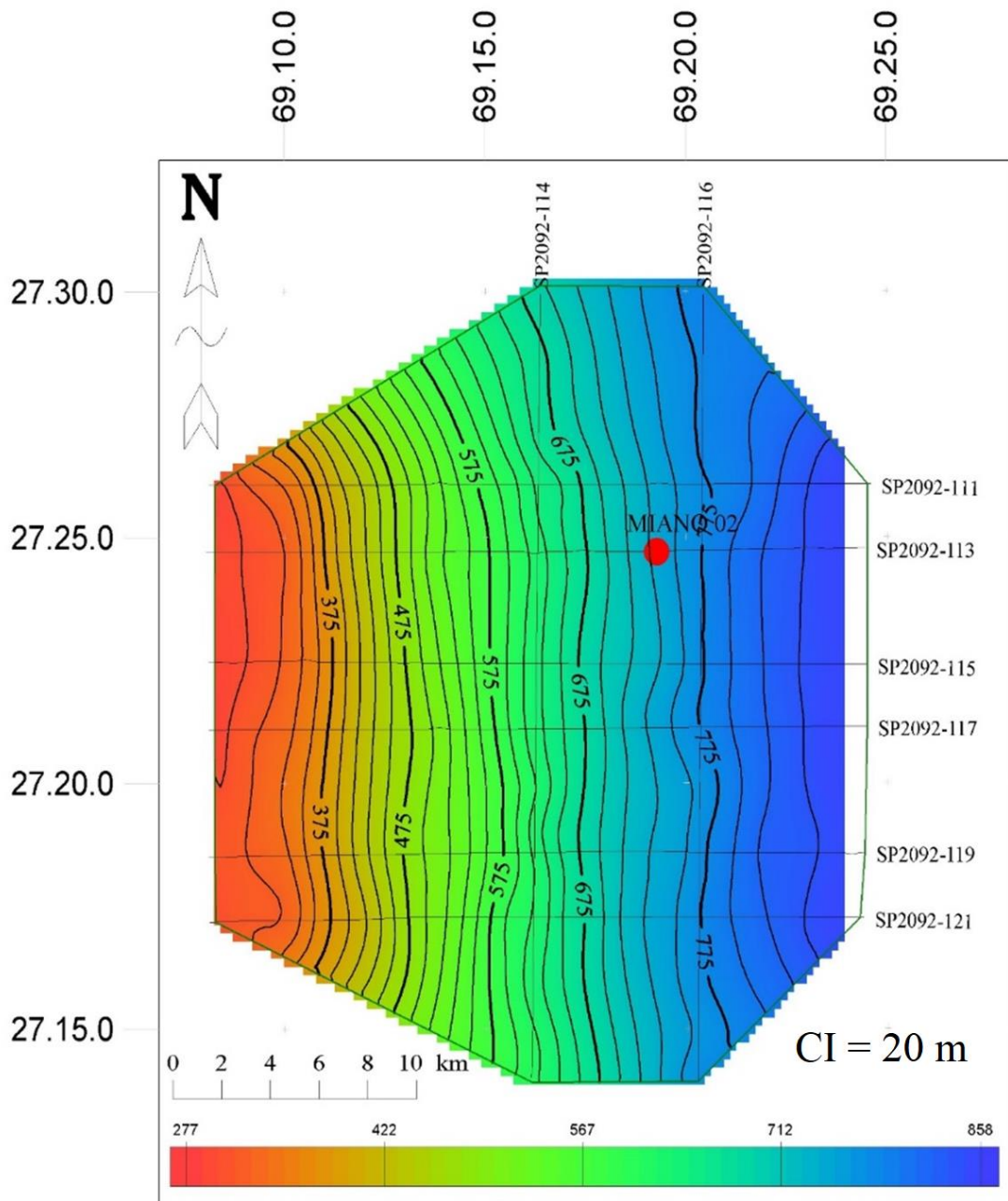


Figure 3.87. Depth Contour Map of Habib Rahi Formation in Miano field.

CHAPTER 4

PETROPHYSICAL ANALYSIS

4.1 Petrophysics

Petrophysical investigation helps us identify the fluid that is occupying the rock pores while also determining the qualities of the reservoir rock. Petrophysical analysis is crucial to the petroleum industry since it is a crucial tool for both hydrocarbon exploration and reserve assessment of any reservoir zone. The main petrophysical characteristics of shale are its volume, its density porosity, the neutron porosity, as well as the average porosity and effective porosity, and lastly, calculation of saturation of water and hydrocarbon. The lithology of the encountered rock unit can also be roughly estimated by professionals using the petrophysical analysis.

Petrophysics analysis is a measurement-based analysis that uses well data as its primary source of information. This analysis is done to figure out how many large units or little units of a particular physical wise there are in a formation or lithology. This study can establish per-depth at much lower scales. values at particular intervals of depth. The following are a few of these analyses: Shale content in a rock is indicated by the volume of clay (Vcl), which is a representation of the shale volume (Vsh). Petrophysics describes the physical properties and behavior of rocks, soils. It mainly focuses reserves of reservoirs. Including ore deposits and hydrocarbon reservoirs. Some key properties studied in petrophysics include the investigation of lithology, porosity, water saturation, permeability and density. Based on its magnitude, pore pressure can be classified as either normal (hydrostatic) or aberrant (overpressure or under pressure). Numerous issues, including kicks, blowouts, wellbore instability, hole washouts, and loss of drilling mud circulation, can result from overpressure. So, for a safe and profitable drilling, accurate pore pressure prediction is required.

4.2 Wireline Log Interpretation Workflow

The following methodology shown in figure 4.1 has been adopted to calculate the parameters required for performing petrophysical analysis. In the petrophysical analysis, log curves like GR, RHOB, PHIN and DT are used to identify the lithologies that are being encountered while moving deeper/downward. By looking at the basic trends of logs like GR, which tells about the radioactive content in Formation also tells us about the amount of clay present in the Formation.

On the basis of percentage of the clay content in the Formation we can name the Formation as CLEAN or DIRTY Formation. Volume of shale can also be carried out by using GR log. It is important to find out the volume of shale because it helps in computing fluid content, formation porosity and Formation permeability. Major concerned porosities are Average Porosity and Effective Porosity. Effective porosity is the total number of pore spaces that are interconnected and can transmit the fluid content in it. Water saturation is an important parameter used in reservoir modelling, as it gives an idea of the percentage of the pore spaces occupied by water and oil or gas and hence the total amount of hydrocarbon present in the pore spaces of the reservoir. Next step is the Hydro Carbon saturation which is important for reserve estimation and reservoir characterization of any oil or gas reservoir.

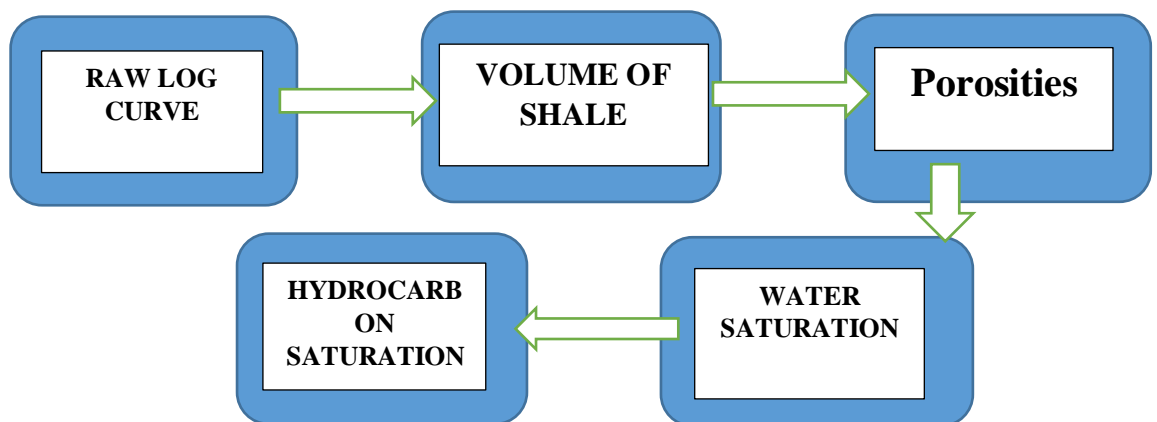


Figure 4.1. Petrophysical Analysis Workflow adopted for the study.

4.2.1 Volume of Shale (Vsh)

The gamma ray log is useful in identifying the presence of shale beds and determining their volume during log analysis. When quantitatively evaluating the shale content, it is assumed that other radioactive minerals are not present. The volume of shale can be calculated using both the gamma ray and spontaneous potential logs. This calculation is important in analyzing the reservoir properties of rocks. The formula for calculating shale volume using the gamma ray log is applied in this study.

The volume of shale in a formation can be calculated using the gamma ray log, which helps to identify and estimate the shale content during log analysis. The gamma

ray log assumes that any radioactive minerals present in the formation are exclusively found in the shale beds. The volume of shale can be determined using both the gamma ray and spontaneous potential. This information is useful in analyzing the reservoir properties of the rocks. The formula for calculating the volume of shale is:

$$V_{sh} = \frac{GR_{log} - GR_{min}}{GR_{max} - GR_{min}}$$

4.3 Porosity

The porosity is defined as the number of pore spaces in the rock. Following porosities have been calculated using the wireline log data of Miano-02 well.

4.3.1 Density Porosity

The formation density log is a porosity log that determines the formation's bulk density using electron density. Using this log, the experts examine complex lithology, hydrocarbon density, minerals, gas-bearing zones, evaporates, and minerals. When high density porosity values range from 60 to 80%, washouts are present. The formula used for calculation of density porosity is as follows:

$$PHID = \frac{\rho_{ma} - \rho_b}{\rho_{ma} - \rho_f}$$

Where,

PHID = Density porosity of the rock

ρ_{ma} = Density of the rock matrix

ρ_b = Bulk density of the formation

ρ_f = Density of the fluid occupying the pores

4.3.2 Sonic Porosity

The sonic porosity, a measure of porosity, determines the elastic wave velocity through a specific lithology. It is calculated by the following equation:

$$PHIS = \frac{\Delta t - \Delta t_{ma}}{\Delta t_p - \Delta t_{ma}}$$

Where,

PHIS = Sonic porosity

Δt = Transit time in the formation of interest

Δt_{ma} = Transit time through 100% of the rock matrix

Δt_p = Transit time through 100% of the pore fluid

4.3.3 Average Porosity

The average is the calculation of number of pore present in the formation. porosity is important for accumulation of hydrocarbons. Average porosity is calculated by using the values of neutron and density logs which provide the information about the number of pores present (Glover, 1998). The average porosity is calculated using following formula:

$$APHI = (NPHI + DPHI) / 2$$

Where ,

Average porosity the average porosity

APHI= Average porosity

NPHI = Neutron porosity

DPHI = Density porosity

4.3.4 Effective Porosity

The effective porosity (ϕ_E) is the proportion of interconnected pore spaces that have the potential to hold recoverable hydrocarbons compared to the total volume of the rock. To determine the number of connected pores in the rock, a calculation is done for effective porosity (ϕ_E), which is the product of the total porosity and the volume of clean material ($1 - V_{sh}$). This calculation eliminates non-connected pore space that is made up of clay.

$$EPHI = APHI \times (1 - V_{sh})$$

Where ,

EPHI = effective porosity

APHI= Average porosity

V_{sh} = Volume of shale

4.4 Saturation of Water and Hydrocarbons

Water saturation refers to the proportion of pore space occupied by water in relation to the total pore space. It can be determined using wireline log data or through core analysis and empirical models. Knowing the water saturation is crucial in determining the presence and amount of hydrocarbon reserves in a reservoir. When water saturation is low, it indicates high hydrocarbon saturation and vice versa. Accurate estimation of hydrocarbon saturation is essential for assessing reserves and characterizing reservoirs in oil and gas fields. The remaining fraction of pore space holding oil and gas is known as the hydrocarbon saturation.

$$S_w^n = \frac{a \times R_w}{\phi E^m \times R_t}$$

Saturation of hydrocarbon is calculated by the following formula .

$$S_h = 1 - S_w$$

4.5 Pore Pressure Prediction

In sedimentary strata, hydrostatic pressure and pore pressure are not always the same, with pore pressure often being higher than hydrostatic pressure, a condition known as overpressure. This can lead to drilling risks such as blowouts and kicks if not properly evaluated. To prevent such occurrences, it is crucial to accurately predict pore pressures. The Miano field's pore pressure is analyzed using the Eaton's approach, which is based on acoustic logs. Overpressure is typically caused by the inability of fluid in the pores to escape at a rate that matches silt deposition, with clay being important in preserving pore pressure due to its 0% permeability. To identify clay-rich intervals, clay intervals are calculated and a baseline is created using the GR curve. A line group is manually created on the GR log curve at approximately 70 API to differentiate clay points from non-clay ones. Overburden pressure, also known as lithostatic pressure, is the primary cause of fluid evaporation from pores. Since pore pressure and fracture pressure are often directly estimated from overburden pressure, it is essential to calculate overburden pressure to anticipate pore pressures accurately. The formula for determining the OB

$$OB = \int_0^z \rho(z) \times g \times dz$$

In usual geological conditions, the pressure exerted by a water column from the depth of a formation to sea level is known as hydrostatic pressure, which is calculated based on the density, gravitational acceleration, and depth. When the pore pressure within a formation exceeds this hydrostatic pressure, it is termed as overpressure. Conversely, if the formation pressure is lower than the hydrostatic pressure at a particular depth, it is described as under pressurised. Utilizing the formula, the hydrostatic pressure (HP)

$$HP = \int_0^z \rho_f \times g \times dz$$

A critical step in pore pressure prediction is to create a trend line for normal compaction. This involves the reduction of porosity during mechanical compaction, causing fluid to be expelled from pores due to overburden pressure. For slowly deposited sediments, this results in a typical compaction trend with predictable porosity reduction rates (NCT). Pore pressure refers to the force exerted by fluid within the pore space of a porous structure. Pore pressure prediction is based on Terzaghi and Biot's effective stress law, which states that the fluid pore pressure depends on both the vertical effective stress and the total stress (Terzaghi, K.; Peck, R. at al). Well log data can be utilized in different ways to predict pore pressure, with Eaton's method being a popular quantitative technique (Biot, M. A). Eaton (1975) utilized the sonic transit time of the compressional wave as an empirical relationship in predicting pore pressure.

$$PP = OB - (OB - HP) \times \left(\frac{NCT}{\Delta T} \right)^3$$

Eaton's method is a technique for predicting pore pressure and fracture pressure in a formation. The method involves determining Eaton's index by comparing projected and measured pressure data. The fracture pressure, which is the pressure required to cause mud loss from the wellbore into the formation, can be calculated using the equation, where NCT represents the normal compaction trend line, PP represents the pore pressure in psi, and the exponent value is a representation of Eaton's index below,

where FP is the fracture pressure and ν is Poisson's Ratio (dimensionless).

$$FP = PP + (OB - PP) \left(\frac{\nu}{1 - \nu} \right)$$

4.6 Basic Petrophysical analysis of Miano-02 well

In the raw log curves, track-01 represents lithology logs i.e., Gamma Ray and Spontaneous Potential logs, along with Caliper log. The GR log showed both high and low peaks throughout the borehole depth. In addition, caliper log showed very high values at many depth intervals, which showed that the phenomenon of 'caving' was present at many parts of the borehole.

Cavings are a major contributor to wellbore instability and can cause up to 40% of downtime in drilling operations. Although they result from rock failure, they do not always lead to instability but can cause problems with clearing debris from the well. Shale shakers can be used to interpret the downhole environment by examining induced cavings, which provide insight into the nature and location of instability. The causes of cavings include underbalanced drilling, stress relief, pre-existing weak planes, and mechanical action during drilling. (Kumar et al., 2012). Track-02 displays the MSFL, LLS, and LLD resistivity logs. Throughout the depth of the borehole, deviations in the resistivity logs' logarithmic representations could be seen. Additionally, at some levels, there was little to no difference between MSFL and LLD. Some zones, however, revealed a distinct separation between MSFL and LLD. Track-03 shows porosity logs i.e., Neutron and Bulk Density logs. Gas effect has also been shown in this track where a cross-over formed between neutron and density log curves, resulting from low values of both. The formation's high concentration of hydrogen atoms, which is a sign of good porosity, is indicated by the formation's low neutron log value. Additionally, a low-density log value shows the porosity of the formation.

4.6.1 Uninterpreted log curves

Petrophysical analysis was performed in the First log curve from 3260m till 3440m. Depth interval of 20m was taken in this log and scale of each log will be defined when discussed. In the first track trend of GR, SP and CALLIPER is observed. Log curve of GR is shown with red line and Scale of GR is taken from 0- 200 API. Initially the curve shows normal behavior but as it progresses it shows fluctuation toward both

ends. Highest value of GR is observed on four points i.e. 3303m, 3208m, 3356m and 3415m whereas minimum value is observed on 3280m, 3308m and 3352m. Log curve of SP is shown with Green line and scale is taken from -100-50 MV. In the initial part of the log the graph drops toward the lesser value and abrupt change in the trend towards positive side at 3280m indicating change in lithology at this point. But as it progresses it fluctuates a little but remains on positive side. Caliper log curve is shown with dotted line and its scale is taken from 6-16IN. Caliper log curve shows dominant behavior after 3300m depth and keeps fluctuating till bottom but towards the highest value side. In the second track the trends of LLS, LLD and MSFL are shown respectively. All of the log curves show the same trend while moving downward except MSFL at some point. Its value decreases so much at some points that it appears on backup scale. MSFL is shown with Blue line having a scale of 0.2-2000 OHM.

Which shows a decrease in the value initially but then shows a normal trend as it progresses. LLS is shown with a dotted line having a scale of 0.2-2000 OHM in which the values remain in the center as we progress. LLD is shown with a red line having a scale of 0.2-2000 OHM which shows the same behavior as of LLS. Third Track shows the log curve of RHOB, PHIN and Gas Effect. PHIN is shown with a Blue Dotted line having a scale of 0.45 - -0.15, which shows an increase towards the positive side initially till 3300m and then shows a trend towards the negative side except at a depth of 3340m. RHOB is shown with a red line having a scale of 2.0 - 3.0 GM/CC. It shows a rapid decrease and increase in the initial patch till 3280m. Its maximum value reaches at a depth of 3300m and it shows the same behavior as of RHOB as it progresses. Gas Effect can easily be seen in the graph from a depth of 3280m to 3380m and again on 3400m to 3430m. Fourth Track shows the trend of Sonic and DT log. Which is mostly represented in opposite manner. Sonic is shown with a purple line whereas Density log is shown with a black line. Sonic having a scale of 140-40 US/FT, which shows behavior towards the lesser side or towards the right side of the curve. It reaches to the lowest value at two points i.e. 3300m and 3330m, whereas DT log curve having a scale of 0.250 - - 0.250 GM/CC which shows behavior opposite to the Sonic Log.

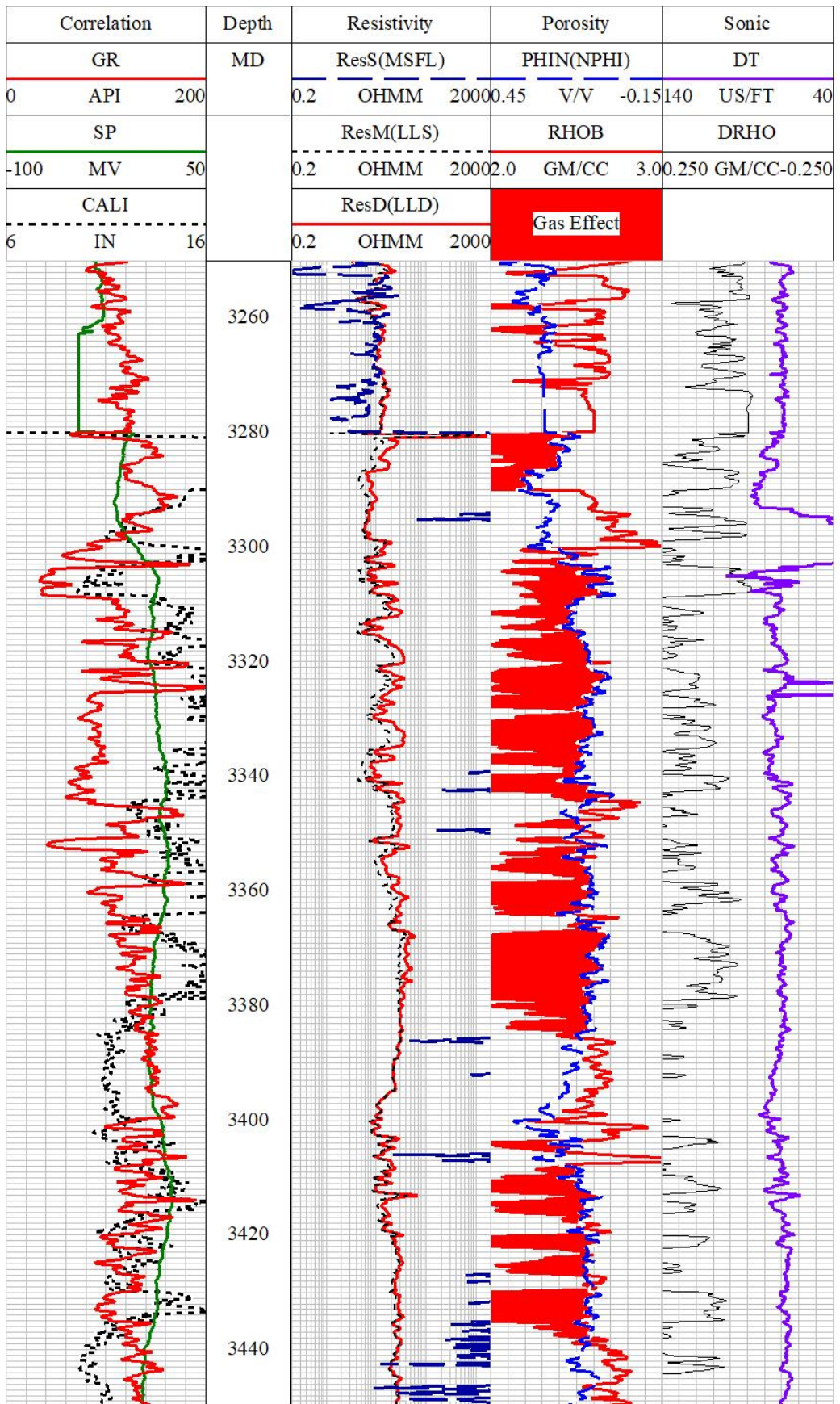


Figure 4.2. Uninterpreted raw log curves of Miano-02 well.

4.6.2 Petrophysical Results

Figure 4.3 shows the log trend of volume of shale, PHID, PHIA, PHIS and PHIE. Volume of shale fluctuates in the log trend. It shows dominant behavior in the path of 3250m to 3290m. afterwards Sandstone dominates at the depth interval of 3300m to 3370m. but in the last patch of 3391m to 3440m volume of shale again dominates. Log curve of PHID is displayed with light grey color having scale of 0 -1. It shows maximum behavior towards left side which is lesser side. Maximum value is observed at some point like at depth of 3290m and in the patch of 3208 to 3270m. next track shows the log trend of PHIA displayed by light green color having scale of 0 – 1. This log curve also shows the behavior toward lesser side but some point like at the depth of 3285m shows some peak.

Next track shows the log curve of PHIS displayed with light blue color having scale of 0 – 1. It also shows same behavior as of previous logs i.e. towards lesser side. Next track shows the log curve of PHIE displayed with light purple color. This curve shows minimal value as compare to previous log that is towards lesser side. Last track shows the percentage of water and hydrocarbon with increase in depth. Water dominates till the depth of 3300m but after that Hydrocarbon shows clear dominates till the depth of 3385m. from this depth till the last point i.e. 3440m some spikes of Hydrocarbon can also be seen but water dominates in that patch. Track-04 shows the curve for Sonic log.

A curve for density correction, known as DRHO, has also been added to this track in order to test the reliability of the bulk density, also known as RHOB. If DRHO is less than 0.15, then the data from RHOB is reliable. However, we observed bad borehole conditions, so the values of RHOB were unacceptable for the calculation of effective porosity, the values of sonic porosity were used instead. The uninterpreted raw log curves have been shown in figure 4.2. In petrophysical analysis, various parameters such as porosity, fluid saturation curves, and lithology are computed using raw log curves with common curve scales. The porosities are represented in fractions using a scale of 0-0.3, while lithology and fluid saturation are plotted on a range of 0-1. A visual representation of these curves can be seen in Figure 4.2.

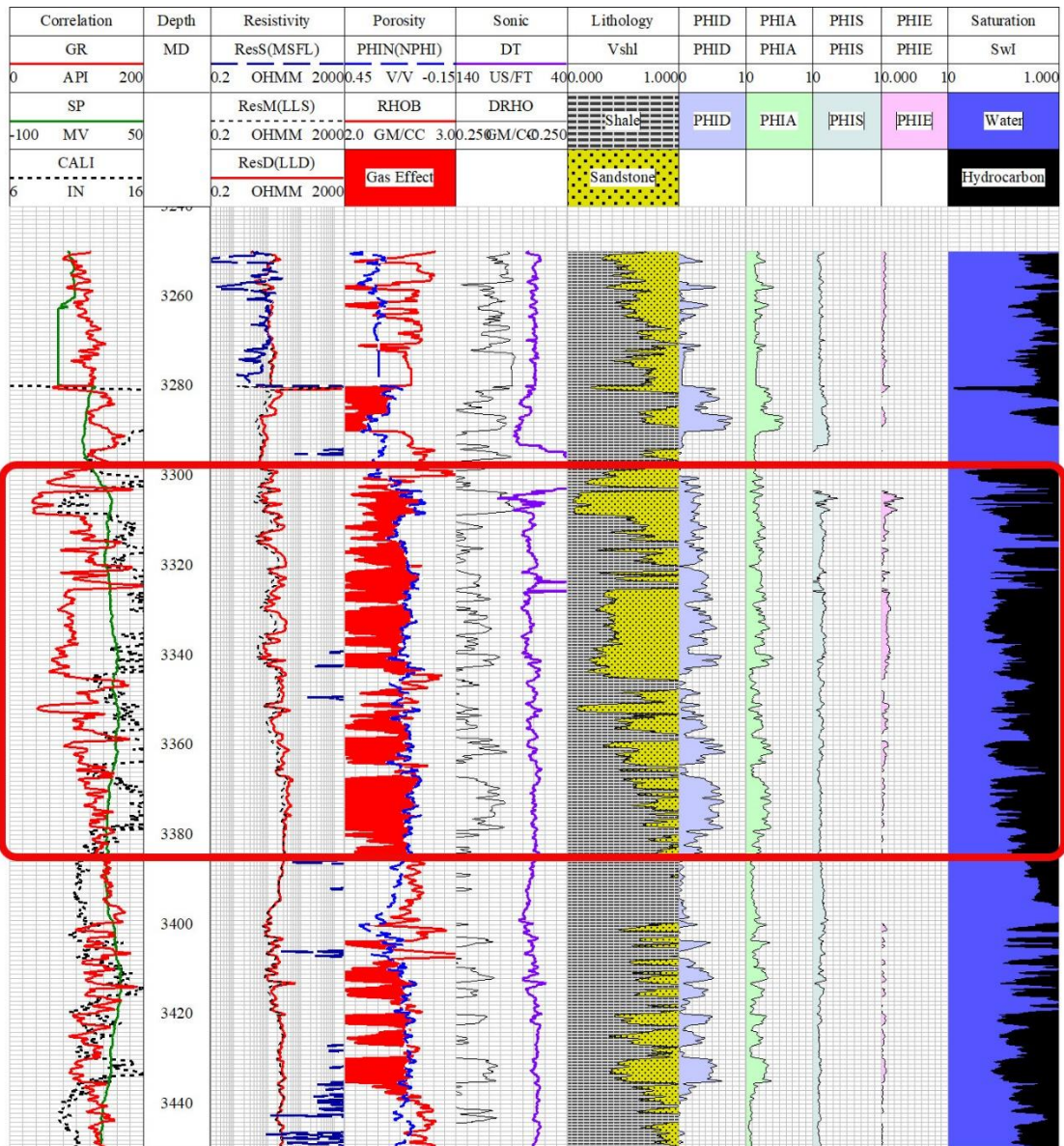


Figure 4.3. Petrophysical Interpretation of Lower Goru Formation showing the zone of interest.

4.11 Pore Pressure Prediction

Figure 4.4 shows the trend of GR, LLD, Sonic; DT, PHIS and pressure conditions. This log curve shows behavior of trends from depth of 2300m till 3500m with interval of 100m. first track shows the behavior of GR while increasing in depth. It is displayed with red line having scale of 0 – 200 API. Almost constant behavior is shown till the depth of 2600m after that increase in the value starts and reaches towards the maximum value at the depth of 3100m. this shows gradual change in the lithology with increase in depth. After the 3100m there is slight decrease in the value but the overall trend is towards the right side.

At the depth of 3500m there is abrupt change in the GR value shows change in lithology at that depth. LLD log curve is displayed with dark blue color having scale of 0.2 – 20000 OHM. It shows a constant behavior towards the lesser value side till 2800m after that slight increase in the log curve is observed with increase in depth Third log curve represents the trend of Sonic and DT which is displayed with purple line having scale of 140 – 40 US/Ft. it also shows constant behavior. Initially The log curve remains in center but starts to dips towards the lesser side as the depth increases. DTNCT line is displayed with red line shows constant behavior throughout.

Fourth track shows the value or log trend of PHIS having scale of 0 – 1. It shows log trends toward lesser side with some peaks in it at some points. Last track shows the value of Hydrostatic Pressure, Over Pressure and Pore Pressure. Hydrostatic pressure displayed with solid dark blue line having scale of 0 – 5000. Its behavior remains same throughout with no peaky nature and slight increase in the value is observed as the depth increases. Value of the Hydrostatic pressure remains towards lesser side. Over Pressure is being represented by Green line having scale of 0 – 5000. Initially the log curve starts from center with very less peaks in it but as the depth increases the value of the Over Pressure increases, also at some point it shows a maximum value or very spiky nature at some depths. That represents the increase in over pressure condition at that depth.

Pore Pressure is represented by solid Red line having scale of 0 – 5000. Initially its log curve starts from left side that is toward lesser value side but at 2390m depth its value decreases abruptly till zero. After that small patch it again reaches towards the previous point and shows constant value with spiky nature till 3300m depth. Some spikes that is towards the lesser side is also observed at different depths but remains constants towards the center. From the depth of 3305m the abrupt increase and decrease in the value of pore pressure can be observed in the last patch of 200m. at the depth of 3300m, 3400m and 3500m it shows almost zero to null value of pore pressure. But it also shows highest peak value after the depth of 3500m.

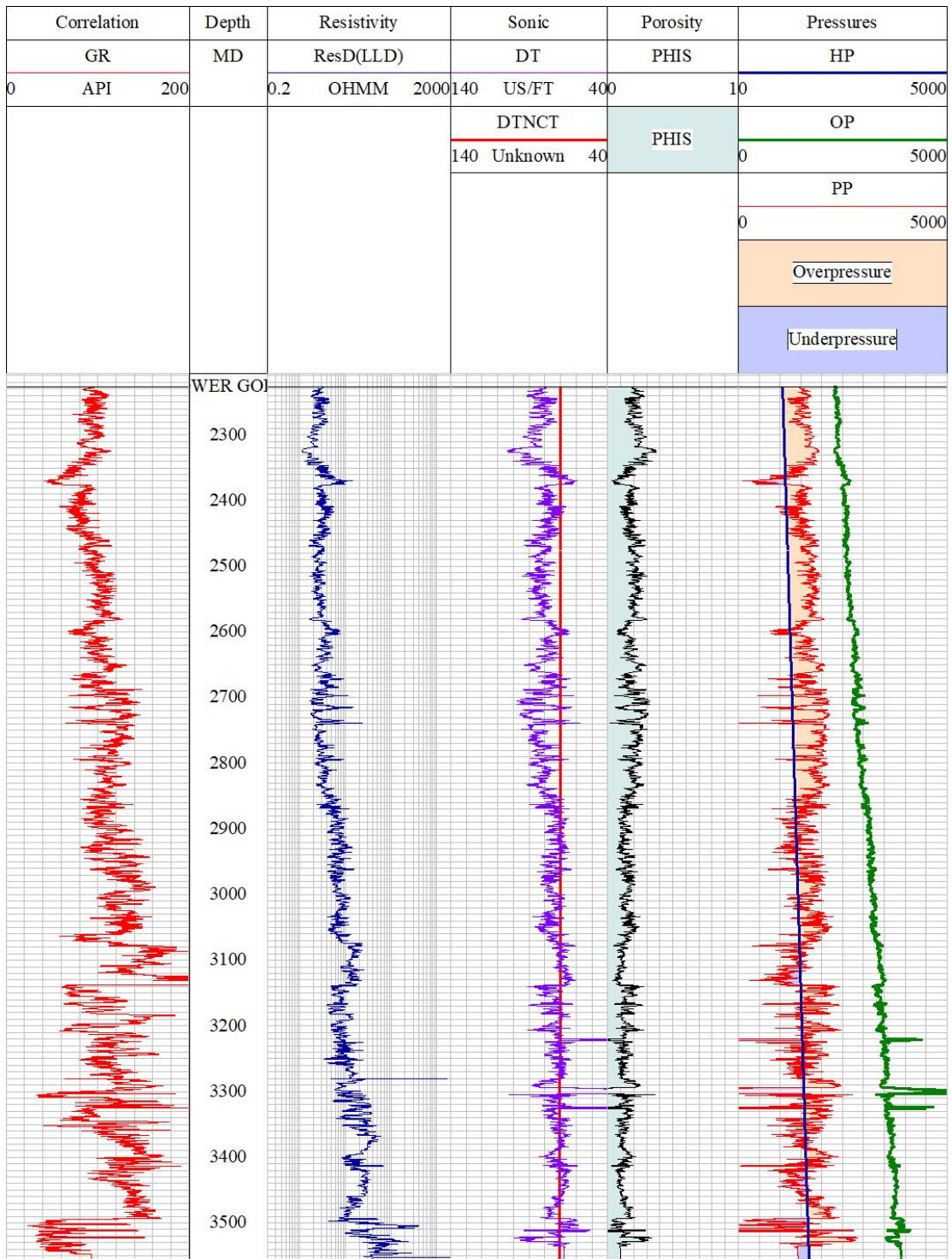


Figure 4.4. Estimation of pore pressures conditions in the Lower Goru Formation.

4.7 Summation Table

The interpreted petrophysical properties and results of pore pressure predictions have been summarized in the summation table given in table 4.1 and 4.2 respectively for Miano-02 well.

Table 4.1. Summation table of Petrophysical Results of Miano-02 well.

Parameters	Average Values
Vsh	44%
Vsand	56%
PHID	27%
PHIN	12%
PHIS	11%
PHIA	19%
PHIE	5%
Sw	48%
Sh	52%

Table 4.2. Summation table of Pore pressure prediction Results of Miano-02 well.

Parameters	Average Values
HP	1382 psi
OP	3103 psi
PP	1937 psi

CONCLUSIONS

- (1) The geological analysis of the area shows that the extensional tectonic activity has resulted in the formation of horst and graben structures through the presence of normal faults.
- (2) The Lower Goru Formation, located at a depth of 3250-3450m, has a highly resistive lowermost layer, and within the interval of 3300-3385m, it contains clean sand with a significant amount of hydrocarbons, making it a promising reservoir.
- (3) The pore pressure assessment indicates that the upper section (2226-3000m) of the Lower Goru Formation has overpressure, which could lead to challenging drilling conditions. On the other hand, the lower part of the formation has normal pressure, making it suitable for drilling.

REFERENCES

- AAPG international conference & exhibition, American Association of Petroleum Geologists (AAPG) (2012)
- Ahmad, S., Alam, Z., and Khan, A.R., 1996, Petroleum exploration and production activities in Pakistan: Pakistan Petroleum Information Service, p.72
- Ahmed, W., Azeem, A., Abid, M.F., Rasheed, A. and Aziz, K., 2013. Mesozoic Structural Architecture of the Middle Indus Basin, Pakistan-Controls and Implications. PAPG- SPE Annual Technical Conference, Islamabad, Pakistan, 1-13. In: Jadoon, S., Mehmood, M., Shafiq, Z. and Jadoon, L., 2016. Structural Styles and Petroleum Potential of Miano Block, Central Indus Basin,
- Bannert, D. and Raza, H. A., 1992. The segmentation of Indo-Pakistan Plate. Pakistan Journal of Hydrocarbon Research.
- Bender, F.K. and Raza, H.A., 1995. Geology of Pakistan, Gebruder Borntraeger, Berlin, Stuttgart.
- Bowers, G. L. Pore pressure estimation from velocity data: Accounting for overpressure mechanisms besides undercompaction. SPE Drill. Completion 1995, 10, 89–95.
- Dobrin, M.B., 1988. Introduction to Geophysical Prospecting, McGraw-Hill Book Company, Tokyo, 629p.
- Dobrin, M.B. and Savit, C.H., 1988. Introduction to Geophysical Prospecting, 4th Ed., McGraw-Hill Book Company, Tokyo, 867p.
- Eaton, B. A. The equation for geopressure prediction from well logs. In Fall Meeting of the Society of Petroleum Engineers of AIME; OnePetro, 1975.
- Fatmi, A. N., 1977, Mesozoic. In Ibrahim Shah, S. M. (ed): Stratigraphy of Pakistan. Geol. Surv. Pak. Mem. 12: 29- 56
- Gallant, C., Zhang, J., Wolfe, C. A., Freeman, J., Al-Bazali, T., & Reese, M. (2007, November). Wellbore stability considerations for drilling high-angle wells through finely laminated shale: a case study from Terra Nova. In SPE annual technical conference and exhibition. OnePetro.
- Glover, D.P., 1998. Petrophysics. University of Aberdeen, 65-150.
- Iqbal, M., Nazeer, A., Ahmad, H. and Murtaza, G., 2011. Hydrocarbon exploration prospective in Middle-Early Cretaceous reservoir in the Sulaiman Fold Belt, Pakistan. PAPG-SPE Annual Technical Conference, P 107-109.

- Kadri, L.B., 1995. *Petroleum Geology of Pakistan*, Pakistan Petroleum Limited, Ferozsons (pvt) limited.
- Khan, M.R., 1994. Aquathermal Pressuring cause for abnormally high pressures encountered in Lower Goru shale/sand sequence in deep drilled well in Central Indus Basin. *Petroleum Seminar*, Karachi.
- Kumar, D., Ansari, S., Wang, S., YiMing, J., Ahmed, S., Povstyanova, M., & Tichelaar, B. (2012). PS Real-time Wellbore Stability Analysis: An Observation from Cavings at Shale Shakers.
- Naseer, M. T., and Asim, S. 2017. Continuous wavelet transforms of spectral decomposition analyses for fluvial reservoir characterization of Miano Gas Field, Indus Platform, Pakistan. *Arabian Journal of Geosciences*, 10, 1-20. v.10, p.210.
- Quadri, Viqar-un-Nisa, and Shuaib, S.M., 1986. Hydrocarbon prospects of Southern Indus Basin, Pakistan. *American Association of Petroleum Geologists Bulletin*, v.70, no.4, p. 396-414.
- Radwan, A. E.; Sen, S. Characterization of in-situ stresses and its implications for production and reservoir stability in the depleted El Morgan hydrocarbon field, Gulf of Suez rift basin, Egypt. *J. Struct. Geol.* 2021, 148, No. 104355.
- Raza, H.A., Ali, S.M. and Riaz, A., 1990. *Petroleum Geology of Kirthar Sub-Basin and part of Kutch Basin Pakistan*. *Journal of Hydrocarbon Research*, no. 1, p. 29-73.
- Rider, M.H., 1993. Gamma-ray log shape used as a facies indicator: Critical analysis of an oversimplified methodology, *Interprint*, p.226. In: Hurst, A., Lovell, M.A.
- Raza, H.A., R. Ahmed, S.M. Ali, A.M. Sheikh, and N.A. Shafique, 1989, *Exploration performance in sedimentary zones of Pakistan: Pakistan Journal of Hydrocarbon Research* v. 1/1, p. 1-7.
- Shahid, M., Qureshi, M. A., Ahmad, K. M., Khan, I., and Sohail, U., 2016, Genetic relationship of Pab Formation with Mughal Kot Formation (Upper Cretaceous) in eastern and western Sulaiman Foldbelt: *PAPG/SPE Annual Technical Conference- Pakistan*, P. 121 - 122
- Terzaghi, K., Peck, R. B., & Mesri, G. (1967). *Soil Mechanics in Engineering Practice*, John Wiley & Sons. Inc., New York, 232-254.
- Terzaghi, K.; Peck, R. B.; Mesri, G. *Soil Mechanics in Engineering Practice*; John Wiley & Sons: 1996

- Udo, K.; Akpan, M.; Agbasi, O. Estimation of Overpressures in Onshore Niger Delta Using Wire-line Data. *Int. J. Sci. Res.* 2015, 4, 2780–2784.
- Wang, Z.; Wang, R. Pore pressure prediction using geophysical methods in carbonate reservoirs: Current status, challenges and way ahead. *J. Nat. Gas Sci. Eng.* 2015, 27, 986–993.
- Williams, M. D., 1959, Stratigraphy of Lower Indus Basin, West Pakistan. *Proc. 5th World Petroleum Cong.*, New York, Sec 1, 19: 377-390
- Yassir, N.; et al. Relationships between pore pressure and stress in different tectonic settings. *Mem-Am- Assoc. Pet. Geol.* 2002, 79–88.